

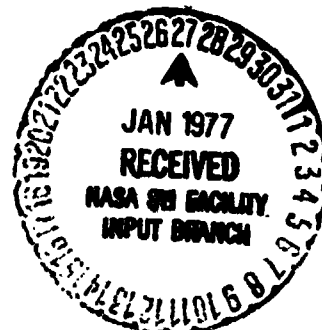
NASA CR-144846

(NASA-CR-144846) OSO-1 FINAL PROGRAM REPORT
Final Report (Hughes Aircraft Co.) 62 P
HC A04/MF A01 CSCL 22A

N77-15062

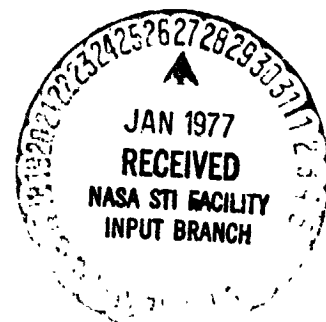
Unclas
G3/15 12306

HUGHES



OSO-I FINAL PROGRAM REPORT

NASA CONTRACT NAS5-11400



REPORT NO. HS331-5239

PROJECT OR PROGRAM NAME ORBITING SOLAR OBSERVATORY (OSO-I)

REPORT TITLE

OSO-I FINAL PROGRAM REPORT

NASA CONTRACT NAS5-11400

DATE DECEMBER 1975

HUGHES

HUGHES AIRCRAFT COMPANY

OSO-I FINAL PROGRAM REPORT

NASA CONTRACT NAS5-11400

CONTENTS

- o INTRODUCTION
- o SUMMARY
- o SUBSYSTEM EVALUATION
 - o Controls Subsystem
 - o Power Subsystem
 - o Thermal Performance
 - o Telemetry and Command Subsystem
- o PROGRAM HISTORY

OSO-8 SIX MONTH ORBIT
PERFORMANCE EVALUATION REPORT

Introduction

The Orbiting Solar Observatory -8 (OSO-8) is in a low near circular earth orbit gathering basic solar and celestial science data. This report presents an evaluation of the spacecraft subsystem performance for the first six months of the mission. Of primary concern is the subsystem performance as related to support of the Observatory experiments. The experiment performance is not presented in detail in this report. The report begins with a performance summary and concludes with a detailed subsystem performance presentation, plus a brief program history.

Summary

The spacecraft subsystems have continued to support the experiments operations as required since the Observatory was launched and established on orbit, June 21, 1975. As of this report, the Observatory has completed six months of on-orbit operations. The experiments are providing high quality science data as they have continued to do so since initial turn-on. The Observatory has been under automatic control of the stored command processor (SCP) since the first few days of initial orbital operations. Without exception, the spacecraft has responded correctly to all properly formatted commands, and has transmitted all tape recorder and real-time data errorlessly. All commanding and data reception problems have been ground system related.

The Observatory was launched aboard the Delta vehicle on June 21, 1975, at 7:43 EDT having been delayed one day because of booster electrical problems. All boost phase events were nominal with Observatory boom deployment, spinup, and separation occurring as planned. The boom backup commands although sent were not required. The Observatory attitude at separation was within a degree of the targeted north ecliptic pole and the spin rate was 4.6 RPM.

During the JOBURG 0 pass the wheel squib driver and OGRA B heater was turned off, and the sail control signal unit turned on as planned. Approximately one hour later over the MILA station, the despin bearing assembly (DBA), nutation damper, and elevation drive assembly were unlocked and the sail despun with PIA directed at the sun via precision sun sensor (SEAS) control. Following this period for the next few weeks, the spacecraft and experiments were checked out. All experiments were gathering science data within the first week after launch.

The primary design goal of maintaining the solar pointed instrument assembly (PIA) pointing stability to within 1 arcsecond has been achieved with a performance of 0.34 arcseconds. Likewise, all other pointing and rastering performance requirements have been satisfied. The on-orbit calibration of the PIA attitude and pointing direction is a continuing task, but present preliminary data indicates the design goals of 5.0 and 30.0 arcseconds, respectively are being attained. The science data obtained by the solar pointed experiments has been outstanding and achievable because of this fine control subsystem performance.

The Observatory spin axis is being precessed along a desired science profile with the magnetic torquer. The axis has been satisfactorily changed with the nitrogen gas system at the planned profile times. The spin axis wobble and nutation is within 0.03 degrees and its attitude is being estimated using star sensor data. The spin rate has been maintained within 6 ± 0.5 RPM. Spin corrections have been executed four times.

In general, spin axis attitude and spin rate control and determination are well within design requirements, thereby allowing the wheel experiments to obtain precise science data. All other control subsystem data is being supplied to the experiments in a satisfactory manner. The initial subsystem configuration with the exception of SEAS A which failed on August 15, 1975, has been utilized throughout the mission. Although SEAS B has continued to support the mission satisfactorily, an unexplainable solar intensity measurement, (telemetry) increase and elevation channel scale factor change has been occurring. This phenomenon is presently being investigated. It should be noted that the CNRS collimator VHF susceptibility problem observed during ground system tests appeared in orbit. The solution to the problem was to use S-band operations whenever the CNRS collimator was active.

The power subsystem has continued to satisfactorily support all experiments and subsystems within design requirements. The subsystem has operated automatically in the configuration established during the initial orbital phase.

The only exception was an unexplainable turn-off of the Wisconsin regulator. It was recommended on and has performed properly without problems.

The thermal performance of the Observatory has been as expected with the exception of the solar panel and DBA. The lower solar panel is running warmer than expected at its peak temperature of 109°C (expected was 107°C) while the upper portion of the solar panel is cooler at the end of the eclipse than expected, -69°C measured, -59°C expected. The maximum measured DBA temperatures of 23 to 29°C exceed expected values by 1°C at the aft bearing to 4°C at the ECRA. These temperatures are below the DBA design limit of 30°C. Temperature difference across the bearings remain small (2 to 3 degrees) and well within the required $\leq 15^\circ\text{C}$.

At this point in time (1 December 1975) the observatory appears to be running warmer than expected but still within appropriate design limits. However, with the approach of Winter Solstice and corresponding short eclipse lengths of 24 minutes it appears that temperatures of many of the subsystems will exceed predicted values from 5 to 8°C. Although some of these subsystem temperatures are expected to exceed design limits none are expected to reach qualification limits. This expected over temperature condition is presently under study.

The telemetry and command subsystems have operated as designed with no anomalies. All spacecraft and experiment data has been recorded and playback or transmitted in real-time as commanded. All commands have been executed and no spurious commands observed. Problems related to commanding, data retrieval, SCP loading, Colorado memory loading, and tape recorder management have been caused by ground system anomalies. With the exception of the first few days in-orbit the Observatory has been under automatic control of the SCP with special tests, events, and tape recorder dumps being interleaved in real time during selected station passes. The SCP is being loaded as many as 4-6 times per day. The initial orbital subsystem configuration is still being used. The recorder B has received the most usage because of the beginning and end of tape operational reliability.

SUBSYSTEM EVALUATION

Controls Subsystem

The excellent performance of the OSO-8 control system is documented herein, and compared with the performance required of the subsystem by the system specification. Additional data are presented which further defines subsystem operation at a level subordinate to the performance requirements, yet serve to detail on-orbit operation of a particular component or which may serve to describe a particular difficulty or failure situation.

Performance Summary

This report covers performance of the OSO-8 control subsystem from launch (day 172 - 21 June 1975) to orbit 2200 (day 318-14 November 1975). The performance of the subsystem has been derived from on-orbit telemetry data, compared with the system specification (SS 31331-100) and the results tabulated in Table I. Wherever possible, the GMT time of the occurrence of the data used to describe performance, is given for cross reference purposes. Extensive comments are also included to assist in the interpretation of the data. Figure 1 through 8 are referred to and serve to augment Table I where required.

In general, performance of the control subsystem has been excellent. The control system has despun the sail night and day, has responded properly to all commands, has automatically sensed day and night transitions, switching from gyro mode to precision sun mode and back to gyro mode, has rastered and offset pointed over the full solar disk, has supported the observatory experiments with inertial reference and timing signals, and has telemetered its sensor information enabling precise spacecraft aspect determination.

The only element of the control subsystem that so far has not yielded trouble free operation has been the SEAS sun sensor. SEAS A failed at GMT 227:18:33:38 during the nighttime portion of Orbit 834, and PIA pointing has been under control of SEAS B ever since. The cause of the failure has been attributed to a catastrophic short within the unit causing the unit's fuses to blow, thereby removing the unit from the non-essential bus. Both sensors have exhibited drifts in their AGC value (the sensor's determination of solar brightness), increasing until the telemetry channel saturated. SEAS B has shown a 5 to 10 percent increase in its scale factor in elevation. Investigations into the possible cause for each of these phenomena are continuing.

SEAS Collimator Performance

The collimator channel of the SEAS sun sensor was intended to measure temperature induced shifts in the experiment telescope and to derive offset pointing commands for the control subsystem so that the experiment telescope pointing could be precisely maintained. Figure 9 illustrates the variation of the collimator outputs during the daylight portion of Orbit 182. SEAS A collimator effectiveness was severely limited by a sensitivity to the spacecraft's VHF transmitter, which appeared to have been related to the wheel booms. Figure 10 illustrates a three cycle per wheel revolution variation in SEAS A elevation collimator output. There was also strong evidence that stray light in the CNRS telescope was causing shifts in the elevation collimator channel of SEAS A over the bottom third of the pointing grid. Unfortunately, SEAS A failed before this problem could be more thoroughly investigated. SEAS B collimator has worked properly since launch, never indicating the EMI and stray light sensitivities of SEAS A.

SEAS AGC Drift

Figure 11 illustrates how the telemetered AGC voltage out of the sensor dipped shortly after launch, and then rose continually until reaching saturation. The telemetry output is buffered from the internal AGC signal by a gain of four. Thus, when TM saturation occurs, there is still 75% of the internal AGC signal's dynamic range remaining. As verified by tests on the Engineering Model SEAS, the normal AGC standardization of the azimuth and elevation channel gain continues. It is obvious, however, that something has caused the sensor to operate in this abnormal AGC region.

In searching for an explanation, attention has centered on the increase in the transmission of light through a thin film (100Å) inconel neutral density filter that covers all sun looking SEAS eyes. Various effects have been investigated: erosion of the filter from micrometeorites and sputtering from charged particles ranging from trapped protons to molecular structures. The latest theory is the conversion of the present filter into a more transparent oxide coating by the chemical reaction of the nickel and chromium with free oxygen. Suffice it to say, that the cause is not yet understood and that investigations continue in an attempt to explain the effect.

SEAS Scale Factor Variations

Figure 12 illustrates the variation of the SEAS azimuth and elevation scale factors since launch. The data shown are from limb measurements made by the pointed experimenters, and from measurements of the large raster retrace motion of the PIA as detected by the gimbal angle sensor. There is a 10% increase in the apparent solar diameter in elevation (according to the experimenters). Azimuth appears to be better behaved. Calibration of the SEAS scale factor and offset by the experimenters was always a part of the operational plan. The rate at which these calibrations must be made, particularly during October, comes as the greatest surprise.

Variation of just the elevation scale factor has not been explained. It may be involved with the AGC drift discussed above or perhaps with differential degradation of the elevation eye with respect to the AGC eye. The problem continues to be explored both at HAC and NASA-GSFC as well as by the experimenters in Boulder, Colorado.

Pointed Experiment Co-Alignment

Data from the pointed experiments places the CNRS telescope boresight above and to the right of the University of Colorado telescope by 35 arcseconds and 15 arcseconds respectively, at the present time. They have seen a shift of about 5 arcseconds in azimuth and 3 arcseconds in elevation since launch.

Nitrogen Gas Leakage

There has been no leakage of nitrogen greater than what can be detected by the 15 PSI pressure transducer telemetry resolution. A very careful review of telemetered pressure and temperature data indicates that gas usage is just what would be predicted for the maneuvers performed so far.

Bus Transients

At a time after dawn, when the solar panel has replenished the battery charge removed during the previous night, the spacecraft bus goes into its "soft" region, where the bus voltage rises with decreasing current demand along the knee of the solar panel characteristic, until the bus becomes limited by the bus limiters. Prior to the beginning of the region, the batteries have been determining the source impedance of the bus, producing a "hard bus" whose voltage will not sag when noise currents are demanded by the load. Similarly, at the end of the region, where the bus limiters determine the bus voltage (providing the load demand is not larger than the limiter current), a "hard bus" is produced. The "soft" region in between can allow a 2 to 3 volt bus voltage variation in response to noisy currents demanded by spacecraft/experiment loads.

The DBA and EDA motors are typical of noisy loads. The situation is worst for the EDA because of the higher gain-bandwidth to SEAS produced noise. The situation is aggravated by large negative pitch angles causing high static EDA currents required to offset flexible cable torque (see Figure 8). Large offsets in elevation or azimuth further aggravate the situation because of angle dependent noise produced in the SEAS. All of these effects were established during system test prior to launch and the necessary protective devices in the electronics deemed adequate to protect the electronics during the transients.

Because of noise current saturation in the EDA and DBA motors (the inductive motor loads driven by constant current drivers are running out of voltage at these high frequencies), insufficient torque is maintained during the "soft" region to maintain PIA pointing. As a result, pointing errors of 4.8 arcseconds maximum observed in elevation and 6 arcseconds maximum observed in azimuth can result, lasting for as little as 16 seconds and as long as 55 seconds. The numbers quoted above were observed during orbit 1912 (299:05:58) when the pitch angle was -4.5° and the elevation offset point was at the extreme of the pointing grid. Less extreme initial conditions will produce less disturbance to the pointing accuracies as evidenced by the problem "going away" once the extreme pitch angle was corrected.

REFERENCE SPECIFICATION 833131-100	PERFORMANCE REQUIREMENT	TABLE 1 OBSERVED ON-ORBIT PERFORMANCE	TIME (GMT)	COMMENTS
3.2.1.1	INITIAL ACQUISITION			
3.2.1.1.1	Initial spin-up - increment ω_p to 5.5 RPM using $\frac{1}{2}$ gas jets.	<p>Booster induced $\omega_p = 4.582$ RPM</p> <p>Two 8 second (50 increment) command sequences initiated. Total spin rate change = 0.986 RPM (from 4.990 RPM to 5.976 RPM).</p>	<p>172:12:19:35</p> <p>172:15:45:10</p>	<p>Initial spin-up delayed until after sail despin and sun acquired.</p> <p>See 3.2.1.1.5</p>
3.2.1.1.2	Solar Acquisition	<p>Satisfactory DBA unlock</p> <p>Satisfactory mutation damper unlock</p> <p>Satisfactory EDA unlock</p> <p>Booster oriented spacecraft to a pitch angle of $\pm 0.78^\circ$</p> <p>DBA motor turn-on</p> <p>Sail despin in 11 seconds</p> <p>Mode 1 125 seconds</p> <p>Mode 2 20.48 seconds</p> <p>Mode 3 10.24 seconds</p> <p>Mode 4 5.12 seconds</p> <p>Mode 5 (in Azimuth)</p> <p>EDA motor turn on</p> <p>Mode 5 sun center</p>	<p>172:13:24:18</p> <p>172:13:25:50</p> <p>172:13:26:35</p> <p>172:12:19:35</p> <p>172:13:25:05</p> <p>172:13:27:54.25</p> <p>172:13:28:08</p> <p>172:13:28:55</p>	<p>No pitch angle correction was necessary</p> <p>DBA motor on command was executed by the spacecraft at the time the spinning SEAS saw the sun (purely a chance occurrence). The sail was travel $\frac{1}{2}$ with the wheel (CCW looking down) at 4.5 RPM. Sail inertial motion ceased 11 seconds later at approximately 1510 of sail angle, CCW wrt the sun LOS. The sail then accelerated in a CW direction back toward the sun, accomplishing automatic (AMS) acquisition in azimuth only. The EDA motor was turned on 25 seconds into Mode 3, and the PIA acquired in elevation in high gain, producing 21 overshoots and requiring 47 seconds. Normal acquisitions take place simultaneously in azimuth and elevation in such a manner as to "ease" the PIA into sun center</p>
3.2.1.2	Day-Night Sensing	<p>Sense day-night at 457.5102</p> <p>Sense night - day at 557.5102</p> <p>Commanded day/night</p> <p>Day/night to experiments</p> <p>Day/night flag to SCF</p>	<p>Averages established from 225:02:51, 225:03:17, 225:03:54, 221:04:18, 204:01:21, 204:01:57, 207:03:13 and 207:04:13</p>	<p>Commanded day/night capability is a backup to the automatic detection of day/night. So far, there has been no need to employ backup spacecraft capability; day/night or the many other backup modes available.</p>

REFERENCE SPECIFICATION SS3131-100	PERFORMANCE REQUIREMENT	OBSERVED ON-ORBIT PERFORMANCE	TIME (GMT)	COMMENTS																		
3.2.1.3 3.2.1.3.1	<p>MODES OF OPERATION</p> <p>Daytime Sun Centered PIA points toward radiometric center of the sun within ± 30 sec over 1 year.</p> <p>The ± 30 sec requirement is met by using the offsets calibrated from on-orbit measurement in a command algorithm which alters the command sent to the spacecraft by an amount necessary to cancel the offset, thereby commanding the PIA to point to the proper place.</p>	<p>Early limb tests indicated that the following commands to the control system placed the optical axis of CNRS on the center of the sun.</p> <table><tr><td></td><td>AZ</td><td>EL</td></tr><tr><td>SEAS A</td><td>-90</td><td>-140</td></tr><tr><td>SEAS B</td><td>+30</td><td>ZERO</td></tr></table> <p>(values in sec)</p> <p>The Colorado Experiment monitored the process but the experiment's internal setup was incomplete at the time, and accurate resolution of the limb was not possible.</p> <p>Recent limb tests indicate SEAS B offsets are:</p> <table><tr><td></td><td>AZ</td><td>EL</td></tr><tr><td>Colorado</td><td>+39</td><td>-39</td></tr><tr><td>CNRS</td><td>+36</td><td>-37.5</td></tr></table> <p>(values in sec)</p>		AZ	EL	SEAS A	-90	-140	SEAS B	+30	ZERO		AZ	EL	Colorado	+39	-39	CNRS	+36	-37.5	174:18:00 Day 318 Orbit 2200	<p>In cooperation with the CNRS Experiment, the control system commands necessary to place the experiment's optical axis on the azimuth and elevation limbs were noted using SEAS A then SEAS B with the collimator disabled. The offset of the control system from the CNRS optical axis was then calculated as follows:</p> <p><u>Neg. CMD (left or up)-Pos. CMD (right or down)-offset</u></p> <p>Command step size in searching for the limb, was limited to 10 sec because of the 10 minute time limitation of a real time OSO pass.</p> <p>Recent offsets obtained with experimenter's "4 corner" limb calibration pointing program. This involves performing a R16S at the +AZ and +EL limbs, and locating the limb with the R16S origin.</p>
	AZ	EL																				
SEAS A	-90	-140																				
SEAS B	+30	ZERO																				
	AZ	EL																				
Colorado	+39	-39																				
CNRS	+36	-37.5																				
	*Large raster centered on solar disk within ± 30 sec	See sun center pointing above.		The same Azimuth and Elevation pointing registers are used for offset pointing as well as rastering. Thus centering of the large raster is equivalent to centering of the offset pointing grid discussed above. Offsets can be compensated for with the command algorithm. The center of the large raster (offset pointing grid) is built into the command generator. Thus the offsets cannot be compensated for. Consequently this specification requirement was waived (waiver #0014553) during system test.																		
		PRODUCIBILITY OF THE FINAL PAGE IS POOR		-9-																		

REFERENCE SPECIFICATION	PERFORMANCE REQUIREMENT	OBSERVED ON-ORBIT PERFORMANCE	TIME (GMT)	COMMENTS																		
3.2.1.3.1 continued	Daytime Sun Centered Stability of pointing, during 1 orbit, shall be $< \pm 3$ sec, 1σ about the mean.	SEAS A outputs <table><tr><td>As</td><td>E1</td></tr><tr><td>15.32</td><td>118</td></tr><tr><td>16.68</td><td>119</td></tr><tr><td>17.82</td><td>120</td></tr></table> Variation over 54 minutes ± 1.3 sec ± 1 sec	As	E1	15.32	118	16.68	119	17.82	120	196:07:45:57 196:08:02:57 196:08:30:09	For the observed data, control was via SEAS B with its collimator enabled. Pointing performance is measured by using SEAS A (without collimator enabled) to monitor SEAS B's control of the sail. Since the performance includes the degradation of both SEAS, telescope pointing stability is better than indicated here. The data was obtained at the beginning, middle and end of the daytime portion of the orbit, a time period of 54 minutes total. Analysis of other orbital data runs indicates that this performance is typical.										
As	E1																					
15.32	118																					
16.68	119																					
17.82	120																					
	Stability of pointing during 5 minutes shall be $< \pm 1$ sec, 1σ about the mean.	The RMS pointing stability within any 5 minute period is $< \pm 0.5$ sec zero to peak, 1σ .	Any orbit (196:08:12:51 for Figure 1)	Figure 1 is a plot of the azimuth pointing error for control on SEAS B with collimator enabled at sun center. During the 1.5 minutes shown in Figure 1, the RMS pointing error is ± 0.34 sec, 1σ . Figure 2 is a corresponding plot of elevation error. Pointing stability is masked by the response of the elevation loop to torque disturbances induced by wobble coupling thru the flexible cable and EDA station restraints.																		
3.2.1.3.2	Daytime Offset Pointed Pointing grid dimension = 44×40 min	Early limb tests with CNRS (see 3.2.1.3.1 above) yielded solar disk dimensions as follows: <table><tr><td>Values in min</td><td>As limb to limb</td><td>E1 limb to limb</td></tr><tr><td>SEAS A</td><td>31.71</td><td>31.42</td></tr><tr><td>SEAS B</td><td>31.59</td><td>31.22</td></tr></table> The nominal solar disk subtends 32 min. The worst case error = -1.82. Recent limb tests yield the following solar disk diameters (SEAS B only): <table><tr><td>Values in min</td><td>As limb to limb</td><td>E1 limb to limb</td></tr><tr><td>Colorado</td><td>32.70</td><td>35.30</td></tr><tr><td>CNRS</td><td>32.70</td><td>35.25</td></tr></table>	Values in min	As limb to limb	E1 limb to limb	SEAS A	31.71	31.42	SEAS B	31.59	31.22	Values in min	As limb to limb	E1 limb to limb	Colorado	32.70	35.30	CNRS	32.70	35.25	174:18:00 Day 318 Orbit 2200	The pointing grid dimensions cannot be measured directly on orbit since they exceed the dimension of the solar disk. The SEAS has been calibrated by pointing to the limbs in azimuth and elevation, using the pointed experiment as the limb detector. Recent limb calibrations of the SEAS indicate the elevation scale factor of SEAS B has been increasing, peaking at $\sim 10\%$ on day 290. SEAS B scale factor is presently stable (See Figure 12). Data reduction has also identified a constant scaling error of the SCSUA raster generator of +1.07% (contributes directly to the 10% SEAS scale factor error percentage)
Values in min	As limb to limb	E1 limb to limb																				
SEAS A	31.71	31.42																				
SEAS B	31.59	31.22																				
Values in min	As limb to limb	E1 limb to limb																				
Colorado	32.70	35.30																				
CNRS	32.70	35.25																				

-10-

REFERENCE SPECIFICATION 5531331-100	PERFORMANCE REQUIREMENT	OBSERVED ON-ORBIT PERFORMANCE	TIME (GMT)	COMMENTS
3.2.1.3.2 continued	Daytime Offset Pointed Point anywhere in grid within command resolution: Azimuth = $1.289 \frac{\text{sec}}{\text{bit}}$ Elevation = $2.344 \frac{\text{sec}}{\text{bit}}$	Experiment data is required to demonstrate conformance to this performance requirement.		
	Accuracy and repeatability of pointing during 1 orbit shall be $< (\pm 3 \text{ sec } +0.4\%)$, 1 σ from the mean for that orbit.	Worst case repeatability error between an upper limb offset point (-175 sec Az , -900 sec El) prior to sunset and the same point, recommended by the control system automatically the next day was 1 sec in Azimuth and 1 sec in Elevation. The time period between data points was 49 min 12 sec. The worst case deviation of the SWS outputs from the command values (after wobble and pointing noise are averaged out) was 2 sec in Azimuth and 3 sec in Elevation.	260:22:26:19	Repeatability and accuracy data were actually taken during a RS reater rather than a fixed offset point because of the lack of data with appropriate offset points held over night, and recommended the next dawn. The specific point chosen was minor frame 52 of the major frame containing the eighth reater line.
	Stability of Offset Pointing During 1 orbit shall be $< \pm 3 \text{ sec}$, 1 σ from the mean during that orbit, established for that fixed offset point.	Typical results at offsets over time periods noted: UP-LT Limb: $\pm 75 \text{ sec Az}$, $\pm 1.25 \text{ sec El}$ for 47 min 35 sec, SEAS B controlling. UP-LT Limb: $\pm 75 \text{ sec Az}$, $\pm 45 \text{ sec El}$ for 18 min 4 sec, SEAS A controlling. Near Center: $\pm 44 \text{ sec Az}$, $\pm 1.53 \text{ sec El}$ for 21 min 10 sec, SEAS A controlling. Worst case observed so far: LO-RT Limb: $\pm 3 \text{ sec Az}$, $\pm 5 \text{ sec El}$ for 42 min 28 sec, SEAS A controlling.	104:12:18:07 107:13:35:51 101:20:39:25 107:15:17:14	Data presented is obtained by using one SEAS to observe how well the other is controlling. Thus the stability of the control system represented by the data includes the stability of both SEAS sensors rather than just the one in control. The collimator readings have been processed with their corresponding control values to obtain net the PIA - Sail movement that occurred during the time period noted. The data are worst case observations and are considered 3 σ quantities when compared to the 1 σ performance requirement.
	Stability of offset pointing during 5 minutes shall be $< 2 \text{ sec}$, 1 σ from the mean during those 5 minutes, established for that fixed offset point.	Stability within any 5 minute period is $< \pm 0.5 \text{ sec}$, 1 σ	Any orbit 107:15:19:25 for Figure 3.	Figure 3 is a plot of Azimuth pointing error for control on SEAS A while pointing to the lower-right limb. During the 1.5 minutes shown in Figure 3, the RMS pointing error is $\pm 0.38 \text{ sec}$ 1 σ .

REFERENCE SPECIFICATION SS31331-100	PERFORMANCE REQUIREMENT	OBSERVED ON-ORBIT PERFORMANCE	TIME (GMT)	COMMENTS
3.2.1.3.3	Daytime Raster Mode *Raster size (total tolerance = $\pm 10\%$) *Large 128 line = $44 \times 39.5 \text{ min}$ (As size x El size) *Large 64 line = $44 \times 39.4 \text{ min}$ *Small 16 line = $2.75 \times 2.34 \text{ min}$ *Small 8 line = $2.75 \times 2.19 \text{ min}$ *Line scan rate = 5.12 seconds and 20.48 seconds per line *Scan lines per raster: *Large = 128 and 64 lines *Small = 16 and 8 lines *Azimuth turnaround: pointing accuracy shall be $0 \pm 1 \text{ sec}$, 10 over 90% of a 40 min Azimuth scan line. This is shown in Figure 4 to be equivalent to a turnaround time of 0.94 seconds maximum.	44.4 x 39.0 min R128S on SEAS B 44.3 x 40.1 min R128P on SEAS A 45.6 x 39.8 min R128F via SEAS B 44.2 x 0 min R64S on SEAS A 43.9 x 36.7 min R64S on SEAS B (0 - see comments) 2.71 x 2.22 min R16P on SEAS B 2.8 x 2.26 min R16P via SEAS A 2.68 x 2.15 min R8S on SEAS B Data synchronized with frame counts, thus line scan rates are correct. Scan line number correct for R122, and R64. Scan line numbers are correct for R16 & R8.	234:09:34:56 204:15:00:24 178:05:48:24 208:01:35:11 196:08:26:44 260:21:48:58 R128:204:14:49:08 to 204:15:00:24 R64:177:07:59:38 to 177:08:21:29 R16: 207:04:10:00 R8:260:21:48:56 204:14:49:08 to 204:15:00:24	Note that "on SEAS A" means control on SEAS A. "Via SEAS B" means SEAS B data, used to monitor control on SEAS A. Data beyond day 227 is just SEAS B data. The day 178 R64 was the only 64 line raster commanded prior to SEAS A failure on day 227. Three separate attempts to process the spacecraft tape dump were unsuccessful in obtaining a complete raster. Thus the elevation size on SEAS A remains unknown. Elevation data, obtained on Day 288 was measured by the Global angle sensor, and indicates a higher than nominal SEAS B elevation scalefactor. There is no data at Hughes for a R8 raster prior to SEAS A failure. Thus there is no SEAS A data to check control on SEAS B. Turnarounds in Azimuth and step-retrace in Elevation occur in synchronism with TM frame times. Figure 5 shows the Azimuth error signal telemetered (Mode 1 TM) at the start of the R128P. In mode 1 TM, this signal is sampled every 0.32 seconds, which accounts for the bandwidth limitation seen in the data. Figure 6 plots Azimuth error vs Elevation error for the worst case turnaround observed in the R128P raster (which turned out to be the 128th line). In all cases, the pointing error has pretty well settled out by the third TM sample which occurs at 0.7125 sec.

REPRODUCIBILITY OF THE SPIN ORBIT POINTING

REFERENCE SPECIFICATION- SS31331-100	PERFORMANCE REQUIREMENT	OBSERVED ON-ORBIT PERFORMANCE	TIME (GMT)	COMMENTS
3.2.1.3.3 continued	Daytime Raster Mode *Repeatability of a programmed point in a raster about the mean position of that point from one raster to the next, c. r. one orbit day shall be $(\pm 3 \text{ sec} + 0.1^\circ)$ 1 σ .	<p>1120P Raster: 1st case two axis repeatability error, one raster to the next = 4.2 sec at a place in the raster (1050, -790 arc) where the allowable tolerance = $\pm 8.3 \text{ sec}$. Control on SEAS A.</p> <p>1165 Raster: Worst case two axis repeatability error, one raster to the next = 3.2 sec at a place in the pointing grid where the allowable tolerance = $\pm 4.3 \text{ sec}$. Control on SEAS B.</p>	<p>Raster I + @ 204: 16:49:08 Raster II @ 204: 15:00:24 Time between points 11:16</p> <p>Raster I @ 192:19:54:58 Raster II @ 192:20:00:26</p>	<p>Eighteen points were chosen over the first 32 lines (available data ends in middle of line 32 of Raster II). The Azimuth and Elevation coordinates of each of these points in Raster I were compared to the same points in Raster II, using SEAS B to indicate how well SEAS A was controlling. The Azimuth and Elevation differences were combined into a two axis error = $\sqrt{(\Delta z \text{ error})^2 + (\Delta E \text{ error})^2}$. None of the eighteen points were out of specification.</p> <p>Sixteen points were chosen over the whole raster. None of these points were $> 3 \text{ sec}$ except for that point noted as worst case to the left. SEAS B was used to monitor PIA pointing.</p>
	*Raster start to be synchronized with the start of major frame	Verified	192:19:54:58	
	*No delay between subsequent small rasters	Verified	192:20:00:26	
3.2.1.3.4	Solar Oriented Night Pointing *Initial Azimuth offset after dusk reset shall be < 0.5 degree, 3 σ , and known to within ± 0.1 degree, 3 σ .	NASA-CSTC, using the variation of MIP location in the spin cycle, has determined total initial Azimuth offset to be 0.1° .		
	*Maintenance of Azimuth nighttime pointing position shall be done by gyro or relative rate mode references. *When on gyro, the drift in Azimuth PIA pointing position from the initial dusk reset Azimuth offset position shall be adjusted so as to not exceed $0.2^\circ/\text{hr}$ (720 arc/hr) during a 10 minute orbit night.	<p>Initial on-orbit drift (uncompensated) = $-0.67^\circ/\text{hr}$.</p> <p>Gyro drift bias of $10.67^\circ/\text{hr}$ commanded. Resulting gyro drift = 110 arc/hr.</p> <p>Last check of gyro drift = 66 arc/hr (former gyro drift bias commanded)</p>	<p>175:20:00:00 175:21:40:00 258:17:33:26 (N3 days later)</p>	<p>Total drift during a 30 minute orbit night, with a drift rate of $70 \text{ arc/hr} \pm 0.01^\circ$</p>

REFERENCE SPECIFICATION 531331-100	PERFORMANCE REQUIREMENT	OBSERVED ON-ORBIT PERFORMANCE	TIME (GMT)	COMMENTS
3.2.1.3.4 continued	Solar Oriented Night Pointing •Relative Rate: residual sail drift rate in Azimuth to be within ± 0.5 RPM of commanded relative rate magnitude.	The relative rate mode, being a backup mode, has never been used on-orbit.	Observations from orbits 20 to 1800	Many samples from 2 days after launch to the present indicate an average DBA friction level of 0.32 ft - lb with a short term (spin period or shorter) variation of ± 0.08 ft - lb about this average. With peak DBA friction of 0.32 ± 0.08 ft - lb, a maximum azimuthal drift rate of 0.4 RPM is predicted, were relative rate mode to be used to control the sail.
	•Elevation PIA pointing to CAS null, $\pm 0.5^\circ$, 3 σ .	PIA caged to $-0.25^\circ \pm 0.08^\circ$ during nighttime.	Observations from orbits 20 to 1800	On orbit data, averaged over orbits 20 to 1800, indicates a nose up flexible cable offset torque of 12.2 oz-in at a gimbal angle of 0° . With a gain of 0.25 ft-lbs/deg. in the night elevation loop, 12.2 oz-in of torque produces a droop = -0.25° . See Figure 7.
3.2.1.3.5	Non-Solar Oriented Night Pointing •Azimuth slew rate = 2 ± 0.40 /sec. on orbit calibratable. Stable to $\pm 3\%$ (± 0.060 /sec).	OCRA slew rate = 2.0730/sec with OCRA A. Regarding stability, 2.0750/sec was measured on this same OCRA almost a year ago in system test.	289:04:12:17	Two 360° daytime slews enabled precise determination of sail rate by measuring the elapsed time between SEAS detected sun crossings.
	•Azimuth acquisition slew rate = 0.8 ± 0.10 /sec.	OCRA B (the cross-strapped backup 2370, required with SC5U A in order to command this rate) has never been turned on since launch. Backup secondary acquisition likewise, has never been attempted.		
	Elevation pointing on CAS reference = (+) and (-) $30 \pm 1^\circ$.	PIA points to -0.25 for a 0° command, $+2.6460$ for a $+30$ command, 2nd -2.970 for a -30 command.	269:10:45:30	Pointing response is consistent with the loop gain measured during system test and a nose up torque, due to the flexible cable electrically interconnecting the EDA and PIA assemblies. Measured values of 12.2 oz-in @ 0° gimbal deflection and a spring term of 2.8 oz-in/deg. are well within Hughes specification values on EDA flexible cable torque: Torque @ Intercept ($\alpha=0^\circ$) ± 16 oz-in Spring Rate ± 4 oz-in/deg.

REFERENCE SPECIFICATION SS31331-100	PERFORMANCE REQUIREMENT	OBSERVED ON-ORBIT PERFORMANCE	TIME (GMT)	COMMENTS
3.2.1.3.5 continued	Non-Solar Oriented Night Pointing Relative rate mode slew rates.	Relative rate mode has not been used on orbit so far.		
3.2.1.3.6	Dawn Acquisitions Upon automatic sensing of sun presence, automatically acquire the sun and resume previous day's pointing activity from any nighttime sail/PJA location, despun or spun.	There have been nearly 2000 acquisitions since the initial acquisition. Of these all but three (see below) were from a despun sun centered nighttime condition. All of the acquisitions were primary acquisitions, all of them successful. No secondary acquisitions have been attempted so far on orbit.	Since launch	
	Total acquisition time between "day" signal and resumption of previous day's pointing activity (mode 5) shall be < 90 seconds when acquiring from a despun sun centered nighttime condition.	Time to acquire (per performance requirement) = 38.4 seconds. Time to acquire initially - from an all spun condition = 169 seconds. Time to acquire from a 166° CCW despun nighttime condition = 91 seconds. Time to acquire from a 290° CCW despun daytime condition = 72 seconds.	Since launch 172:13:28:55 204:01:37:02 289:04:18:05	Angles are measured in Azimuth from sun LOS looking down on spacecraft. Initial acquisition (see 3.2.1.1.2 above) Nighttime pointing activity was to allow CHRS to view the moon. Daytime OGRA slew rate calibration.
3.2.1.3.7	Night Reference System The nighttime Azimuth reference system shall be provided by a gyro whose drift rate shall be capable of being up-dated by command.	Initial gyro drift rate successfully compensated (see 3.2.1.3.4) During moon viewing, CHRS drifted across the moon using the gyro bias at 20°/hr.	175:21:40:00 204:01:25:58	

REFERENCE SPECIFICATION SS31331-100	PERFORMANCE REQUIREMENT	OBSERVED ON-ORBIT PERFORMANCE	TIME (GMT)	COMMENTS
3.2.1.4	ORIENTATION CONTROL			
3.2.1.4.1 and 2	Pitch and Roll Control "Control spin axis to a pitch angle of 0 \pm 40 via ground command."	Pitch angle is being maintained between -40 and +40 using both gas jets and magnetic torquing.	Since launch	
	"Command maneuvers of up to 60 in 3 minutes in increments of 0.25. Maneuvers to be made spun or despun, using wheel sun or MIP reference, night or day, by command. Performance predictions: Jet effectiveness, pitch 0.2080/rev or roll, two jets Cross coupling pitch into roll $\leq \pm 0.0524$ deg/deg roll into pitch $\leq \pm 0.0524$ deg/deg pitch or roll into spin $\leq \pm 0.0035$ rpm/deg	Numerous pitch and roll maneuvers have been made since launch, at night and day, using Y and MIP for the precession references, using only the real SAE and only with the sail despun. Data from the + roll maneuver of 220:17:04:00 indicates the jet effectiveness (ratiored up to 6 RPM) = 0.2070/rev [based on thrust of jet 1 = 0.4 lb, thrust of jet 2 = .39 lb, plume impingement degradation of 16% for jet 2, $I_x = 439$ aft2 and moment arm of 2.935 ft]. Crosscoupling into pitch was 0.058 deg/deg and into spin was 0.0038 RPM/deg. Insufficient detail exists to evaluate the many other maneuvers performed so far. Performance is judged to be completely satisfactory, however.	220:17:04:00	
	"Command maneuvers of up to 2 degrees per day via magnetic torquer system	"> 2 degrees per day easily achieved"		Quoted from Computer Sciences Corporation memo to NASA - GSFC (Contract NAS 5-11999, Task 539).
	"Magnetic field to be 39 ampturn meter ² minimum with the highest current level commanded.	"The milliamperes to pole-cm conversion factor is 565 pole-cm/ma." Note $565 \frac{\text{pole-cm}}{\text{ma}} \times 75 \text{ ma} \times \frac{1}{1000} \frac{\text{amp-turn-m}^2}{\text{pole-cm}}$ = 42.38 amp-turn-m ² at the highest current level commanded.		Quoted from above reference
	"Phase and period clocks to range up to 33 minutes with phase resolution of ± 0.5 minutes and period resolution of ± 0.02 minutes.	"The automatic QOMAC torquing system operates as specified by Hughes Aircraft Company."		Quoted without complaint from above reference

REFERENCE SPECIFICATION SS31331-100	PERFORMANCE REQUIREMENT	OBSERVED ON-ORBIT PERFORMANCE	TIME (GMT)	COMMENTS
3.2.1.4.3	Spin Axis Stability *Spin Frequency wobble shall not exceed 0.1 degree zero to peak	Wobble = 0.022 degree zero to peak	181:18:04:07	Wobble amplitude measured with GAS while PIA is pointing on the sun via SEAS. Predicted wobble amplitude = 0.065° zero to peak, 3σ.
	*Wheel plane excursions, excluding wobble, measured during any 5 minute interval (except during maneuver transients) shall be less than 0.1 degree zero to peak.	Down acquisition transient is the worst case for non gas jet maneuver transients. Initial nutation angle = 0.11° which damps to less than 0.1° in 2 to 3 minutes. Average nutation damper time constant = 147 seconds. Spin rate = 5.97 RPM. Inertia ratio = 1.119 ±0.006	191:20:54:37	A carefull plot of GAS output vs time was made for the dawn acquisition noted (Figure 8). A wobble sinusoid of 0.022° zero to peak beating with another sinusoid whose amplitude was exponentially decaying, was fitted to the plot yielding spinrate, nutation angle, nutation time constant and inertial ratio. The predicted value for the average nutation damper time constant is 165 sec at 5.97 RPM. The observed inertia ratio ($I_z/I_{transverse}$) is only off by 1% from the predicted value of 1.129.
3.2.1.5	SPIN RATE CONTROL *Spin rate to be controlled to 6 ± 1 RPM via ground command	Wheel spin rate being maintained between 5.42 and 6.11 RPM by NASA-GSFC	Since launch	
	*Spin rate corrections of $\pm 0.25 \pm 0.05$ RPM in 1 minute. Performance prediction: Jet effectiveness, spin up or spin down (two jets) = .00874 RPM increment	Four spin up maneuvers (including initial spin correction) have been performed so far, commanding a total of +1.996 RPM. No spin down maneuvers have been performed. Jet plume impingement on the despun asil occurs as predicted. Jet effectiveness is defined as the change in spin rate per increment. The jet effectiveness averaged over the four spinup maneuvers = 0.00918 RPM/inc. 5% higher than the predicted effectiveness of 0.00874 RPM/inc. The 5% might reflect a higher thrust capability of the spin up jets (5% is within the range of allowable thrust predicted for these jets prior to launch)	172:15:45:00 246:16:09:00 258:02:00:00 266:20:37:00	
3.2.1.6	ASPECT DETERMINATION	Star sensor data is processed by NASA-GSFC for fine spin axis attitude determination.		
3.2.1.6.1	Fine Aspect Determination *Inertial orientation of the spin axis to ± 3 min, 1°, 2 axes.	Day: Y to V over one orbit = 5.6479 ± 0.001 RPM minimum variation ±0.0022 Night: MTP to MTP over one orbit = 5.6489 ±0.001 RPM minimum variation ±0.0022	Fine spacecraft aspect data started 176:12:24:00 and continues to the present	
	*Wheel spin rate to an accuracy of $\pm 0.01\%$, 3°, 6 to 10 RPM, day or night.	Day: Y to V over one orbit = 5.6479 ± 0.001 RPM minimum variation ±0.0022 Night: MTP to MTP over one orbit = 5.6489 ±0.001 RPM minimum variation ±0.0022	Day 263 SNAP 5 data used	-17-

REFERENCE SPECIFICATION	PERFORMANCE REQUIREMENT	OBSERVED ON-ORBIT PERFORMANCE	TIME (GMT)	COMMENTS
3.2.1.6.1	<p>Plane Aspect Determination</p> <p>* Inertial azimuth position of a wheel reference related to TN time to ± 3 min, 1σ during daytime</p>	<p>During ACO 65 real time pass, a 13 major frame, frame dump of words 126 and 127 was obtained from which: average $\dot{\theta}$ to $\dot{\psi}$ spin period = 10.12380 sec. = 5.927 RPM</p> <p>Maximum $\dot{\theta}$ to $\dot{\psi}$ jitter produced ± 0.0000820 sec. variations about this average spin period or $\pm 0.0029^\circ$ (± 0.17 min) of azimuth jitter at this spin rate.</p> <p>Average MIP to MIP spin period = 10.12381 sec. = 5.927 RPM</p> <p>Maximum MIP to MIP jitter produced ± 0.00010 sec. variations about this average spin period or $\pm 0.0036^\circ$ (± 0.21 min) of azimuth jitter at this spin rate.</p>	176:19:53:34 (daytime, sun center pointing)	<p>The daytime wheel reference can be the $\dot{\theta}$ pulse activated by the sun directly or by the MIP pulse which indicates the coincidence of wheel and sail axes; the sail inertially despun on the sun.</p> <p>The $\dot{\theta}$ and MIP jitter values, obtained from $\dot{\theta}$ to $\dot{\psi}$ or MIP to MIP period, can related to individual pulse jitter by holding one pulse fixed in time a let the full jitter value represent the uncertainty in the location of the next pulse. In actuality, both pulses are moving. The jitter quoted is therefore the worst case observed.</p>
	<p>* Inertial azimuth position of a wheel reference related to TN time to $\pm 0.2^\circ$, 3σ during nighttime.</p>	<p>The contributors to this quantity are:</p> <p>a) MIP jitter, measured above as $\pm 0.0036^\circ$.</p> <p>b) Gyro drift, measured at 110 sec/hr maximum after compensation (see 3.2.1.3.4).</p> <p>c) Dusk reset offset, measured as $\pm 0.1^\circ$ (see 3.2.1.3.4).</p> <p>Adding these contributors: $\pm 0.134^\circ$</p>		<p>The nighttime wheel reference is the MIP pulse indicating the coincidence of the wheel and sail axes; the sail inertially despun by the gyro.</p>
	<p>* Inertial azimuth and elevation position of each telescope, with respect to sunline to $\pm (5 \text{ sec} + 0.5^\circ)$, 1$\sigma$, 2 axes, during daytime.</p>	<p>It had been expected that sufficient and accurate knowledge of the relationship between the actual inertial location of the telescope optical axis and the location designated by the telemetered SAS outputs would have been established by the pointed experimenter in time to allow, in this report, conformance with this requirement. In practice, both pointed experimenters use the command value sent to the spacecraft as the absolute reference point rather than the telemetered SAS outputs, when they do their limb calibrations. The CNAS experiment, with its finer resolution, has the greatest potential of calibrating the SAS outputs if desired, although limb measurement d.c. scatter, obtained so far, exceeds the specification on this aspect measurement by 4:1.</p>		

REFERENCE SPECIFICATION 5831331-100	PERFORMANCE REQUIREMENT	OBSERVED ON-ORBIT PERFORMANCE	TIME (GMT)	COMMENTS																
3.2.1.6.1	<p>Fine Aspect Determination</p> <ul style="list-style-type: none">Inertial Azimuth position of each telescope with respect to sunline to $\pm 0.5^\circ$, 3σ, for sun centered nighttime pointing.Inertial Elevation position of each telescope with respect to sunline to $\pm 0.5^\circ$, 3σ, for sun centered nighttime pointing.	<p>Sum of error contributors = $\pm 0.134^\circ$ (see "Inertial Azimuth position of a wheel reference" above).</p> <p>Worst case deviation observed from calibrated PIA position $\begin{cases} +0.015^\circ \\ -0.095^\circ \end{cases}$</p> <p>Knowledge of Inertial attitude $\pm 0.5^\circ$ of spin axis (from star sensor = ± 3 min)</p> <p>Adding these contributors: $+0.065^\circ$, -0.145°</p>	<p>182:09:26127</p> <p>233:04:22:05</p>	<p>The inertial Azimuth position of the PIA is obtained at night from telemetry of the MIP reference pulse.</p> <p>Because of the upward torque on the PIA due to the flexible cable, the 0° command position of the PIA actually droops to -0.25°. This position is considered a known or "calibrated" point, and it is the variations from this point, and it is the variations from this point that contributes to the uncertainty in the inertial telescope position at night. Numerous SNAP 5 printouts were consulted and the worst case deviations reported to the left. Since SNAP 5 data is a record of the instantaneous gimbal angle sensor readings, the values include the worst case combinations of nutation and wobble, sensor non-linearities, sensor calibration stability, EDA bearing station and telemetry errors.</p>																
3.2.1.6.2	<p>Coarse Aspect Determination</p> <ul style="list-style-type: none">Spin Axis pitch angle with respect to the sun LOS to $\pm 0.5^\circ$. Provisions to accomplish measurement spun or despun, using real, pseudo or 800Hz for pitch frequency reference.	<p>The worst case performance of the coarse pitch angle TM readout is compared below to the gimbal angle sensor reading when the PIA was sun center pointed during the day. As a check, the fine pitch angles obtained from the star sensor are also compared.</p> <table><thead><tr><th>Coarse Pitch Angle</th><th>Gimbal Angle</th><th>Error</th><th>Fine Pitch Error</th></tr></thead><tbody><tr><td>2.58°</td><td>-2.66°</td><td>0.08°</td><td>2.52°</td></tr><tr><td>-1.88°</td><td>1.96°</td><td>-0.82°</td><td>-1.94°</td></tr><tr><td></td><td></td><td></td><td>-0.06°</td></tr></tbody></table>	Coarse Pitch Angle	Gimbal Angle	Error	Fine Pitch Error	2.58°	-2.66°	0.08°	2.52°	-1.88°	1.96°	-0.82°	-1.94°				-0.06°	<p>182:12:31:31</p> <p>230:05:42:00</p>	
Coarse Pitch Angle	Gimbal Angle	Error	Fine Pitch Error																	
2.58°	-2.66°	0.08°	2.52°																	
-1.88°	1.96°	-0.82°	-1.94°																	
			-0.06°																	
	<p>Spin axis roll information to $\pm 3^\circ$ day or night</p>	<p>Magnetometer status information and real time data continues to indicate nominal magnetometer operation. Processing of magnetic field zero crossings into roll attitude information is a NASA-GS/C operation presumably largely supplanted by fine star sensor data.</p>		-19-																

REFERENCE SPECIFICATION SS31331-100	PERFORMANCE REQUIREMENT	OBSERVED ON-ORBIT PERFORMANCE	TIME (GMT)	COMMENTS
3.2.1.6.2	Coarse Aspect Determination Wheel spin rate to $\pm 0.5\%$, 2 to 12 RPM, day or night.	Fine spin rate based on the spin period between 7 pulses was compared to the change in SAE count per unit of time over spin rates between 5.49 and 6.09 R.H. The worst case deviations observed were: $\pm 0.48\%$ and -0.35% .	208:01:03:28	The coarse spin rate measurement has been implemented in NASA-GSFC software as the change in the wheel Azimuth data (13 SAE count) telemetered from the spacecraft, per unit time. This was implemented instead of using the coarse spin register so that coarse spin rate data could be obtained night or day without having to command the VIP for the precession reference, and because of the higher accuracy obtainable with this method.
(SS31331-1408 3.1.1.2.4.6)	POINTING LOOP STABILITY MARGINS Provide sufficient stability margins in the various pointing control loops, to assure stable loop operation during mission life, considering tempera- ture and structural properties of the sail and FIA instrument package.	See fine aspect determination - 3.2.1.5.1	All orbits	
3.2.1.7	ON BOARD ASPECT REFERENCE Provide experimenters and SCP with the following signals: a) MIP, V and SAE for wheel Azimuth b) Day/night c) Raster Status.	Sufficient stability margin has been demon- strated by near perfect pointing performance during the 4 months so far in orbit. Control loops employed so far are the high gain Azimuth day loop, the Elevation day loop, the Azimuth (gyro) and Elevation (IAS) night loops, the coarse sun sensor loop and the Azimuth and Elevation dual reference loops. No signs of rigid or flexible body instabilities appear in the pointing error responses, and the transient performance follows closely what was observed during NST, DVT and System Test.		Receipt of signals by all experimenters has been acknowledged as adequate by all experimenters.

REPRODUCIBILITY OF ALL
ORIGINAL PAGE IS POOR

ORBIT 360
 GMT 196:08:12.51
 08:13:00
 15
 30
 45
 60
 75
 90
 276 ft.

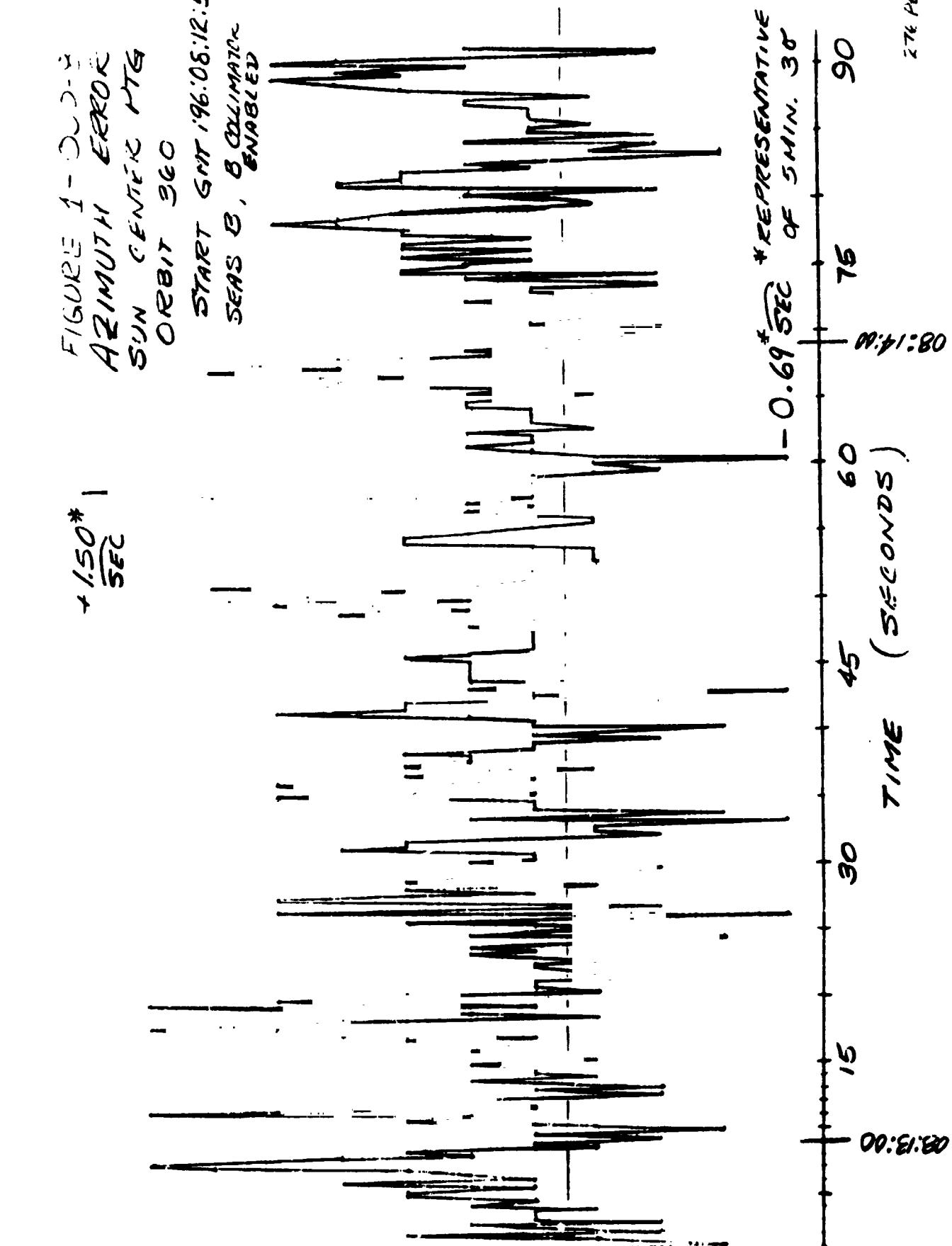


FIGURE 1-000-2
 AZIMUTH ERROR
 SUN CENTER PTH
 ORBIT 360
 START GMT 196:08:12:51
 SEAS B, COLLIMATOR
 ENABLED

+1.50*
 SEC

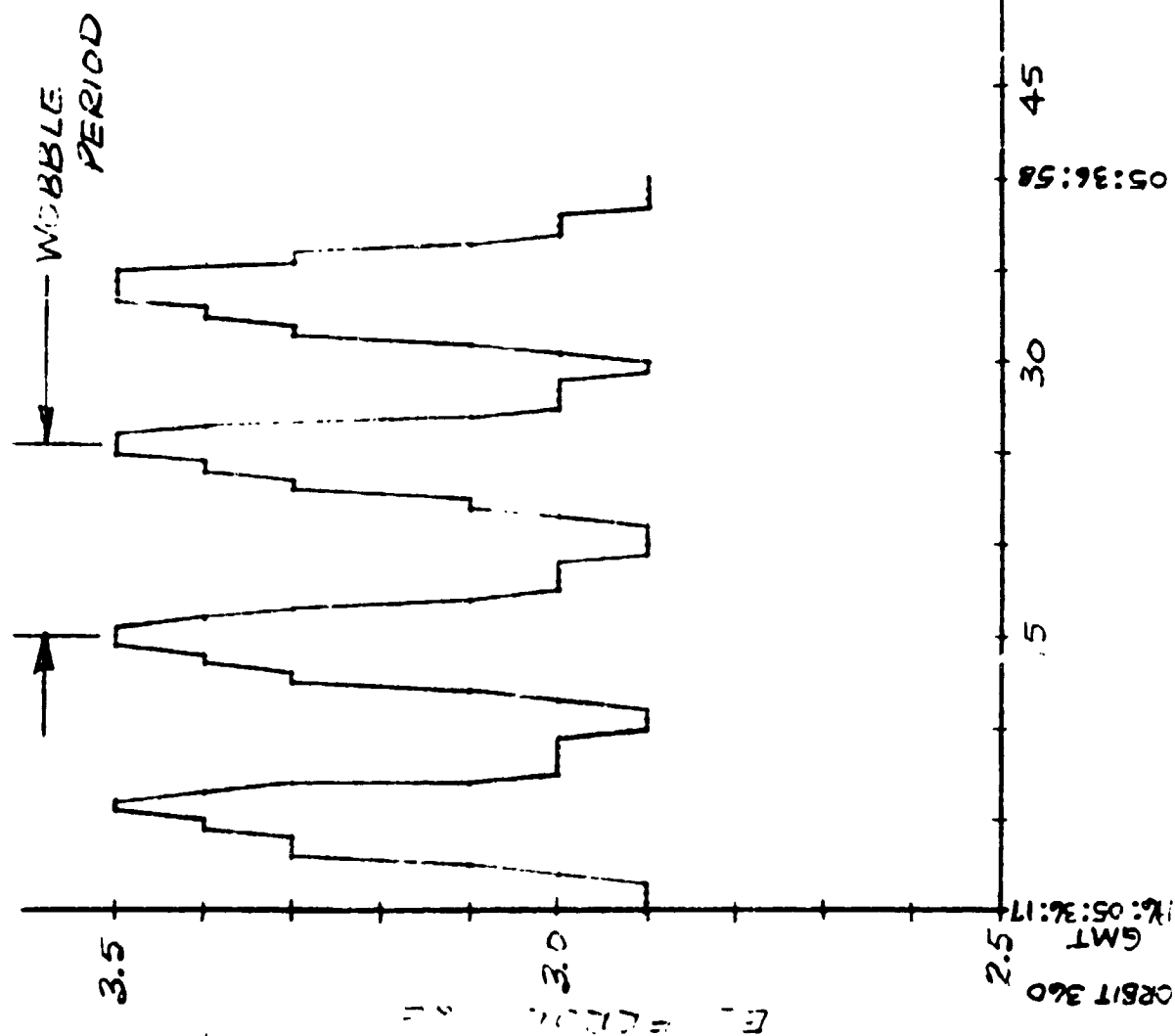
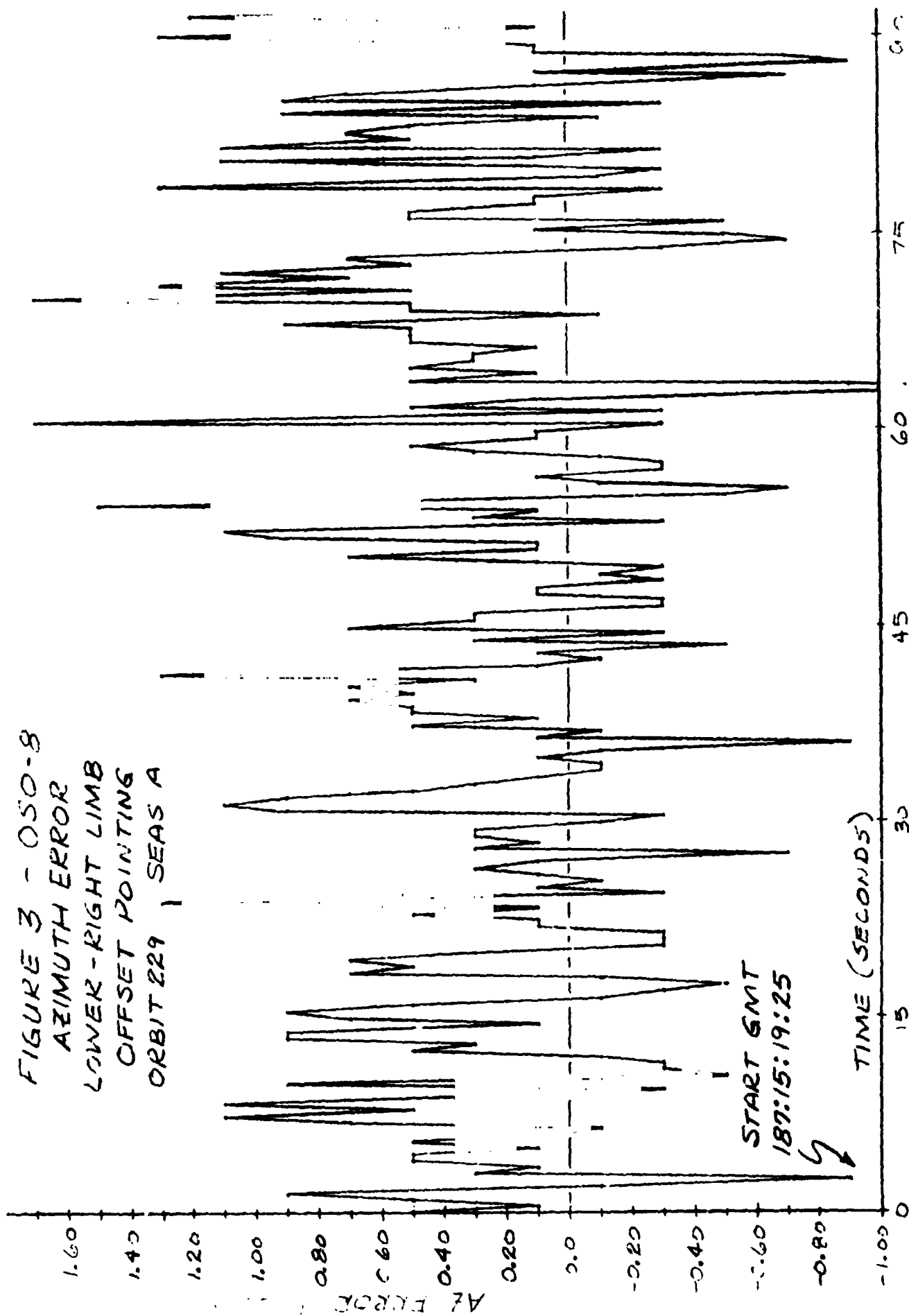


FIGURE 2 - OSO-8
 ELEVATION ERROR
 SUN CENTER POINTING
 ORBIT 360
 START GMT 196:08:12:51
 SEAS B, B COLLIMATOR
 ENABLED
 PITCH ANGLE = -2.4°
 SPIN RATE = 5.98 RPM

REPRODUCIBILITY
 RECAL PACT L. POUH



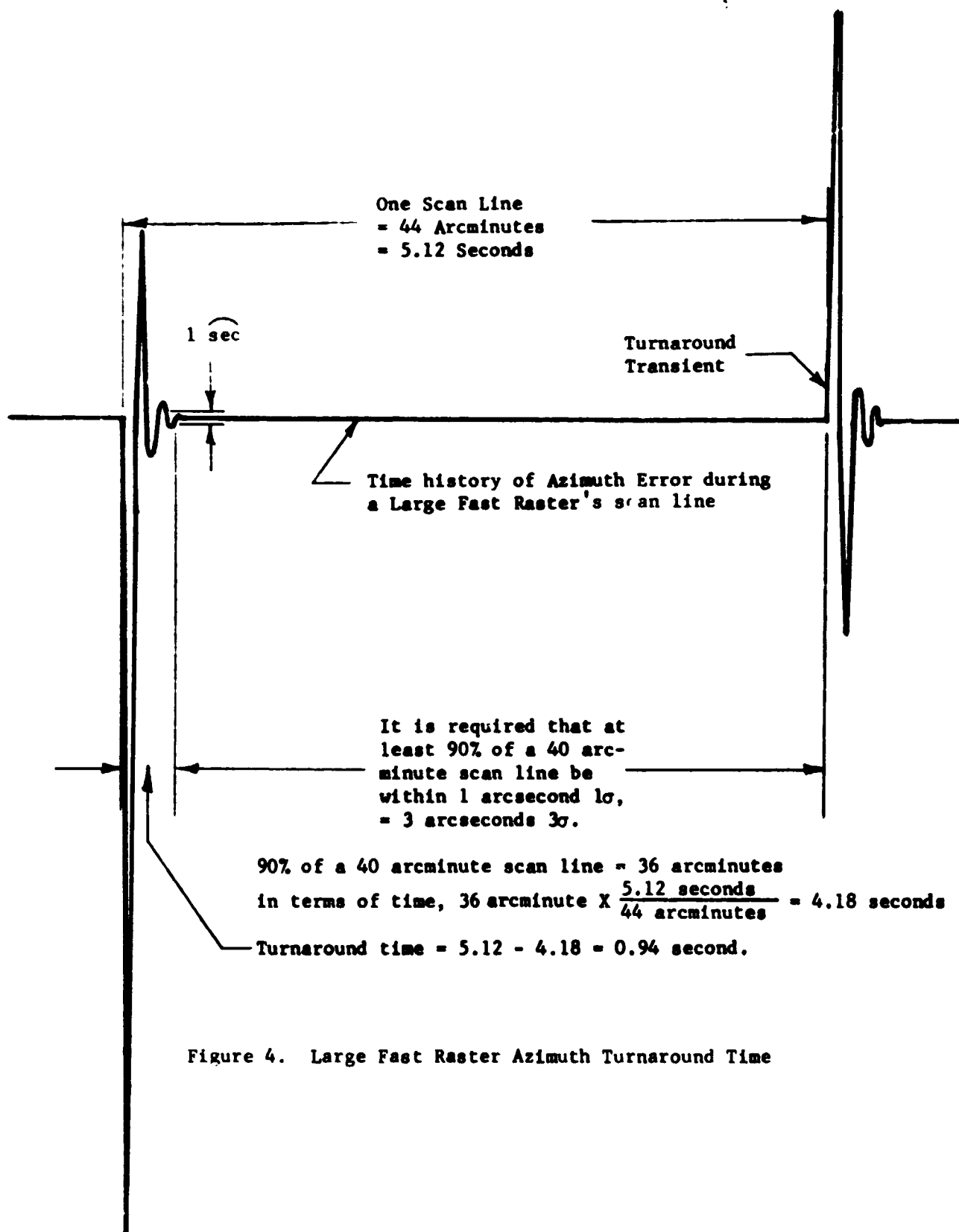
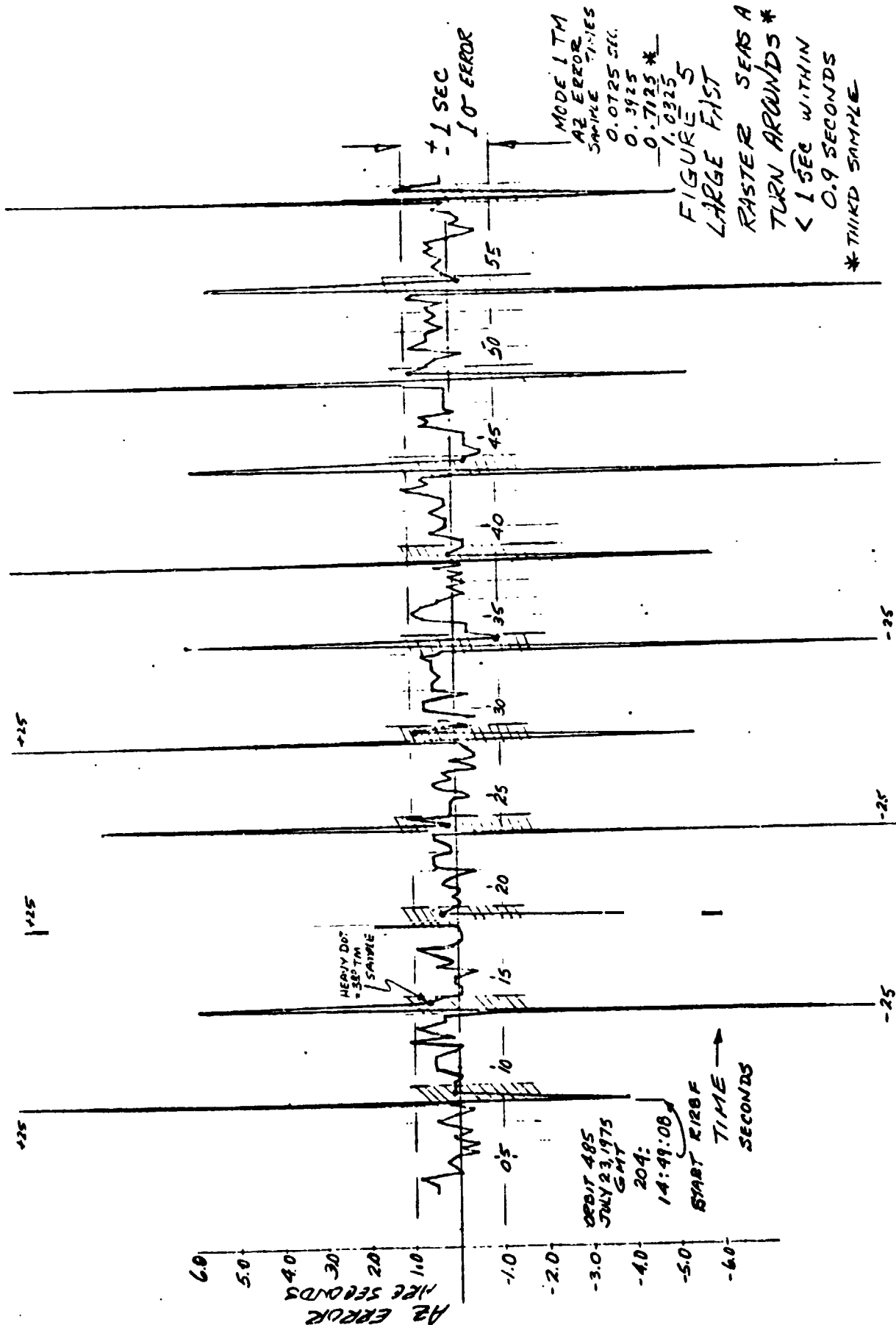
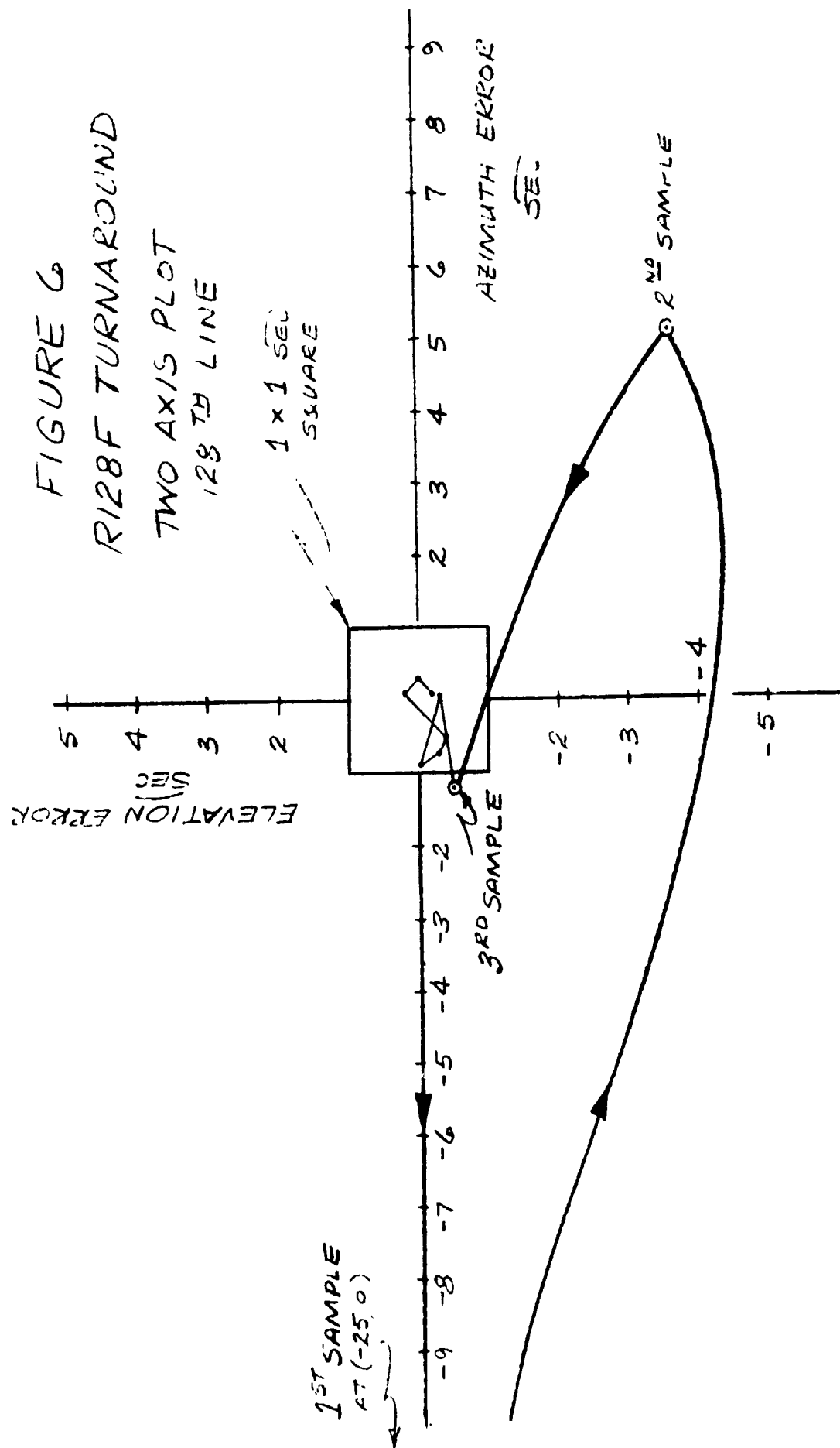
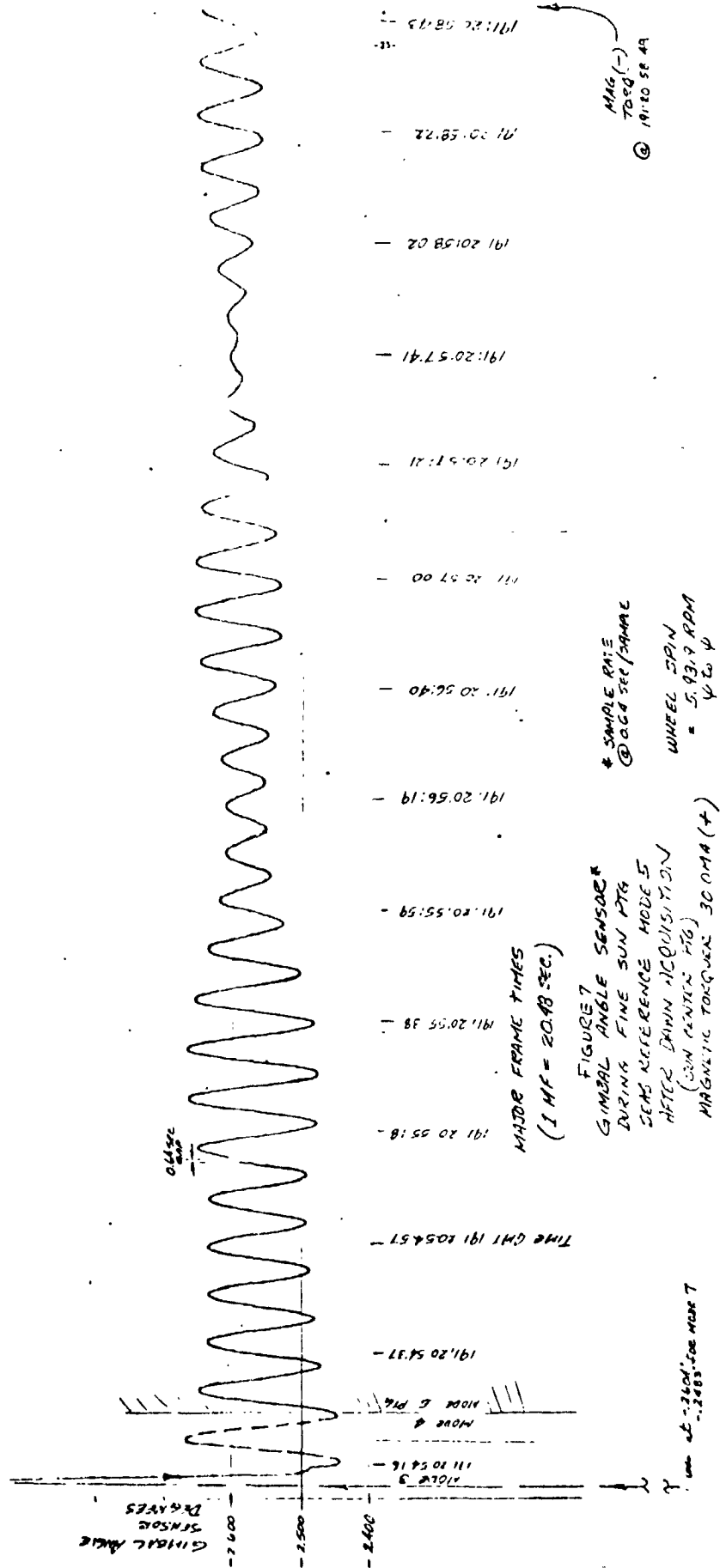
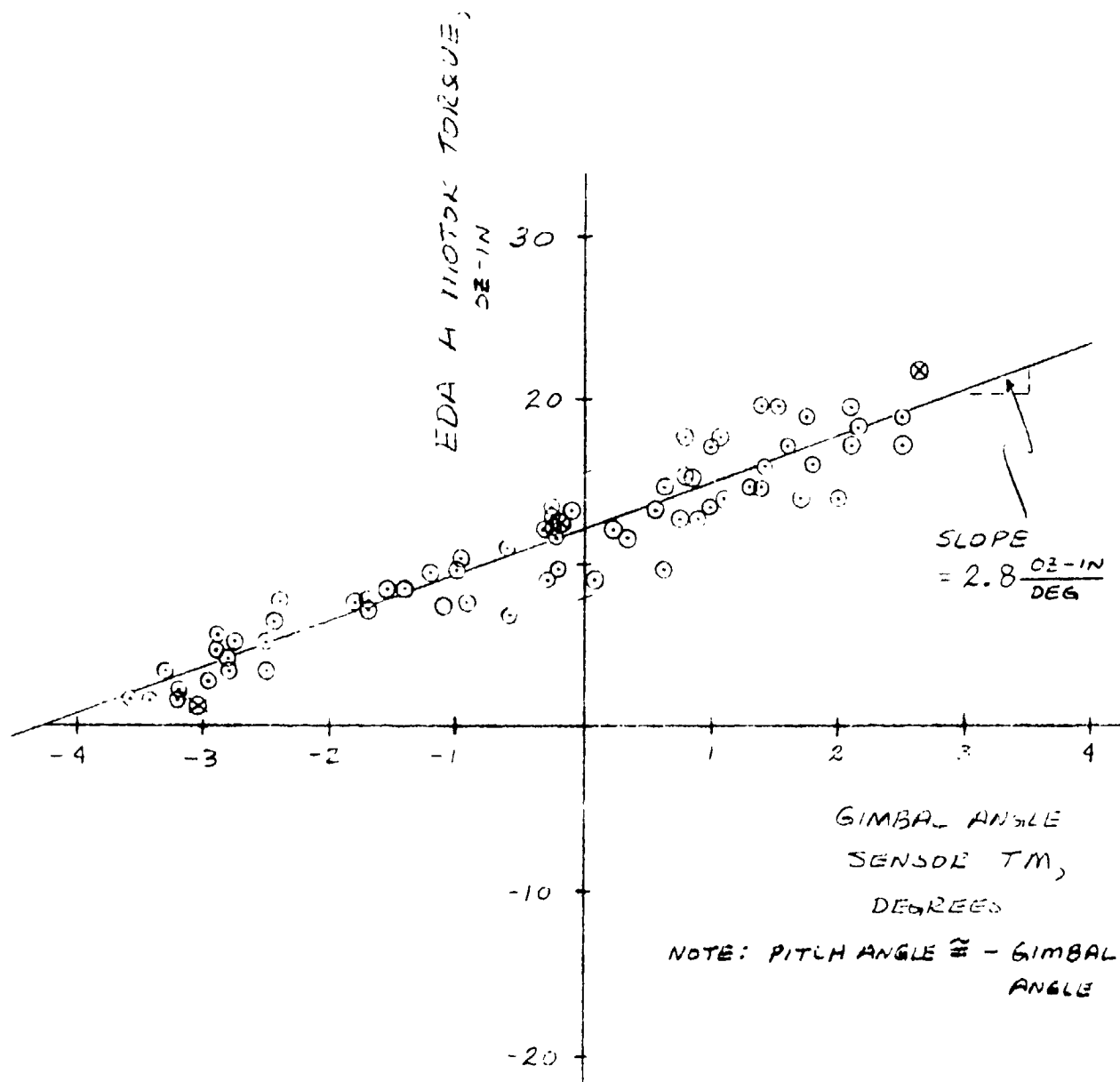


Figure 4. Large Fast Raster Azimuth Turnaround Time





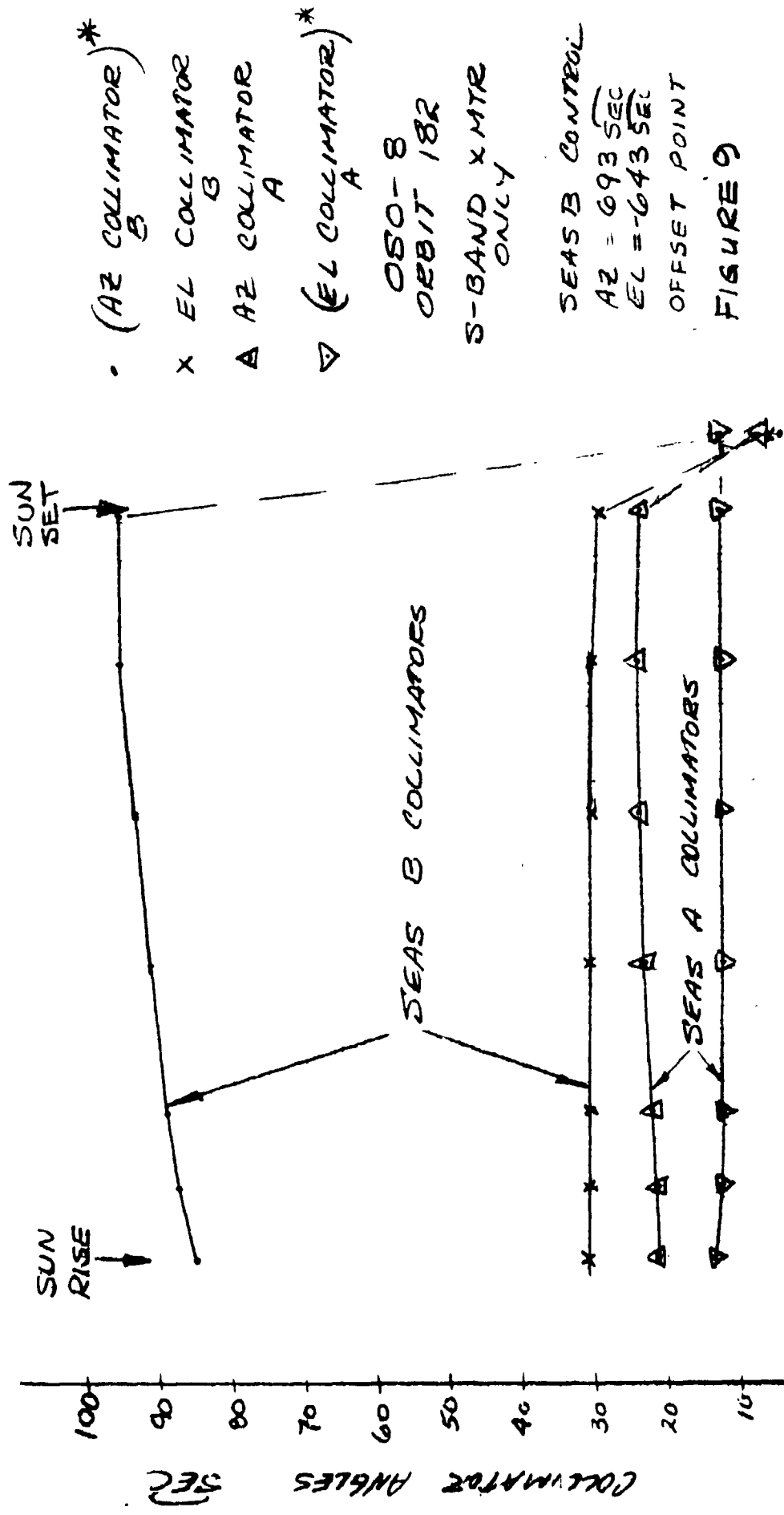




○ AGGREGATE OF DAYTIME DATA OBTAINED OVER ORBITS 20-1800,
OVER VARIOUS SPACECRAFT PITCH ANGLES.

⊗ NIGHT POINTING DATA: $-3^\circ, 0^\circ$ & $+3^\circ$ (267:10:45:30)

FIGURE 8
EDA MOTOR TORQUE/GIMBAL
ANGLE CHARACTERISTIC



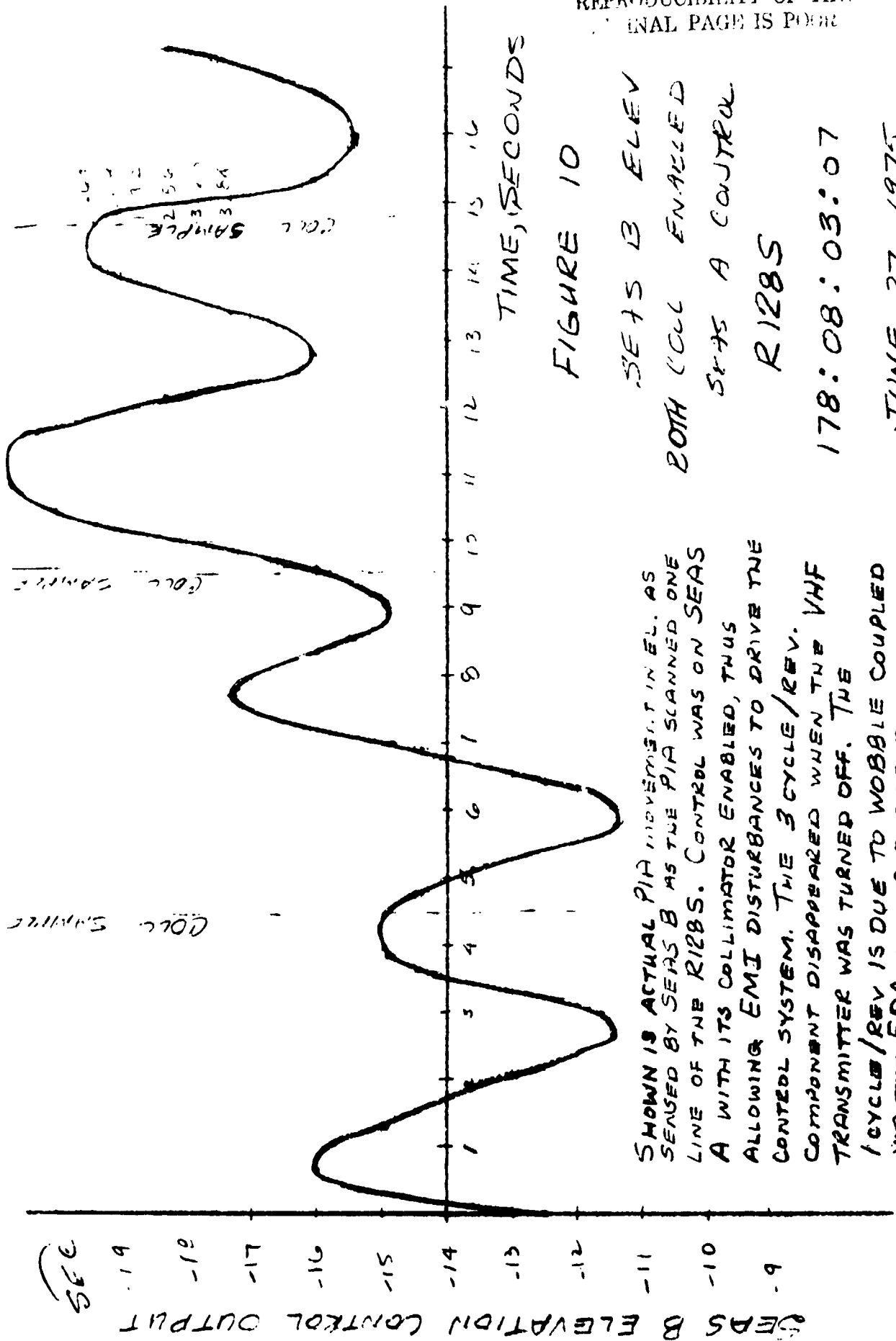
184:12:10 GMT

184:13:00

184:13:00

TIME (MINUTES)

* MULTIPLY COLLIMATOR ANGLE VALUES BY -1



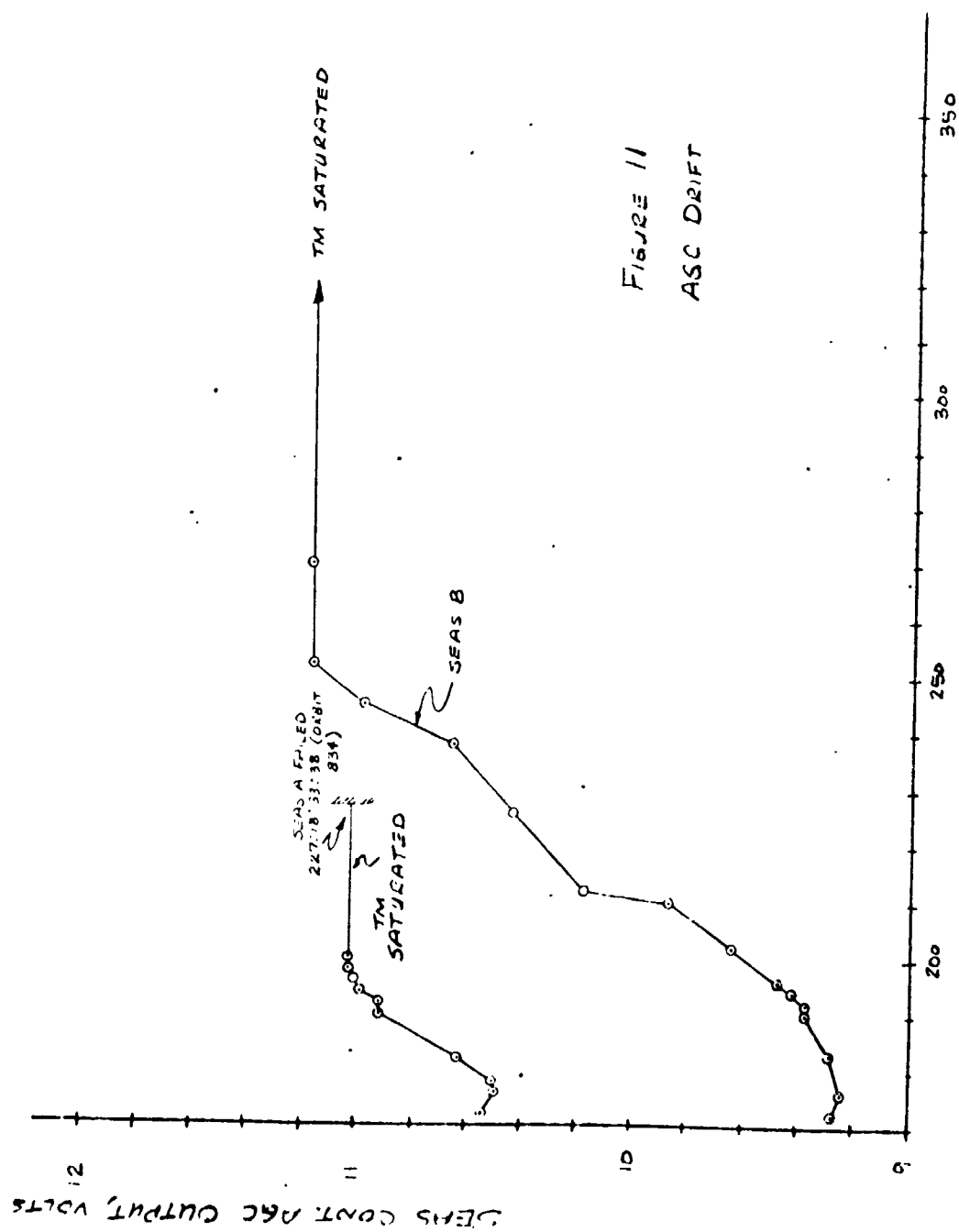


FIGURE 11
ASC DRIFT

JULIAN DAY, 1975

Power Subsystem

The observatory was launched at summer solstice when solar intensity is at a minimum level. At that time there was adequate solar panel current available. The margin at the beginning of the mission was at least 20% during the longest eclipse and there should be no problem to support the spacecraft and experiment loads for at least two years.

After sixty days in orbit solar intensity had increased by approximately 2%. Panel degradation due to radiation during this time was also approximately 2%. Therefore, solar panel output remained essentially constant. Panel voltage, current and temperatures are continuously changing over a full orbit as shown in Figure 13.

The average solar panel voltage before battery clamp is reached is approximately 30 volts. The preflight predicted solar panel current at this voltage during summer solstice at beginning of life was 14 amperes. From Figure 13 it can be seen that the actual measured solar panel current was very close to this value.

Solar panel temperatures near the end of day at the bottom of the panel reach a maximum value of 105.4°C. This is approximately 10°C above the nominal predicted value. For this reason the current at this time, at a bus voltage of 33 volts, is approximately 0.5 ampere below the predicted value. However, by this time the battery charge controllers have clamped the battery voltage and excess panel capacity is being dissipated in the bus limiters anyway.

Solar panel temperatures of the top and bottom sections are plotted in Figure 13. The top temperature sensor measures the back side of the panel; the face side is approximately 14°C higher.

Battery performance during the first six months in orbit was excellent. During the first three weeks in orbit eclipse times were short and the battery voltages were clamped very early in each orbit day. To prevent overcharge, charge currents were rapidly forced down to approximately 0.25 amperes at end of day.

After nine days in orbit, eclipse time decreased to 24 minutes. As a result, the orbital average battery temperatures slowly rose to a peak value of 21.6°C. Battery temperatures decrease to a minimum value when the eclipse time reaches a maximum value of 36 minutes. Figure 14.

APPARENT SOLAR DIAMETER (AS SEEN BY SEAS B), MIN

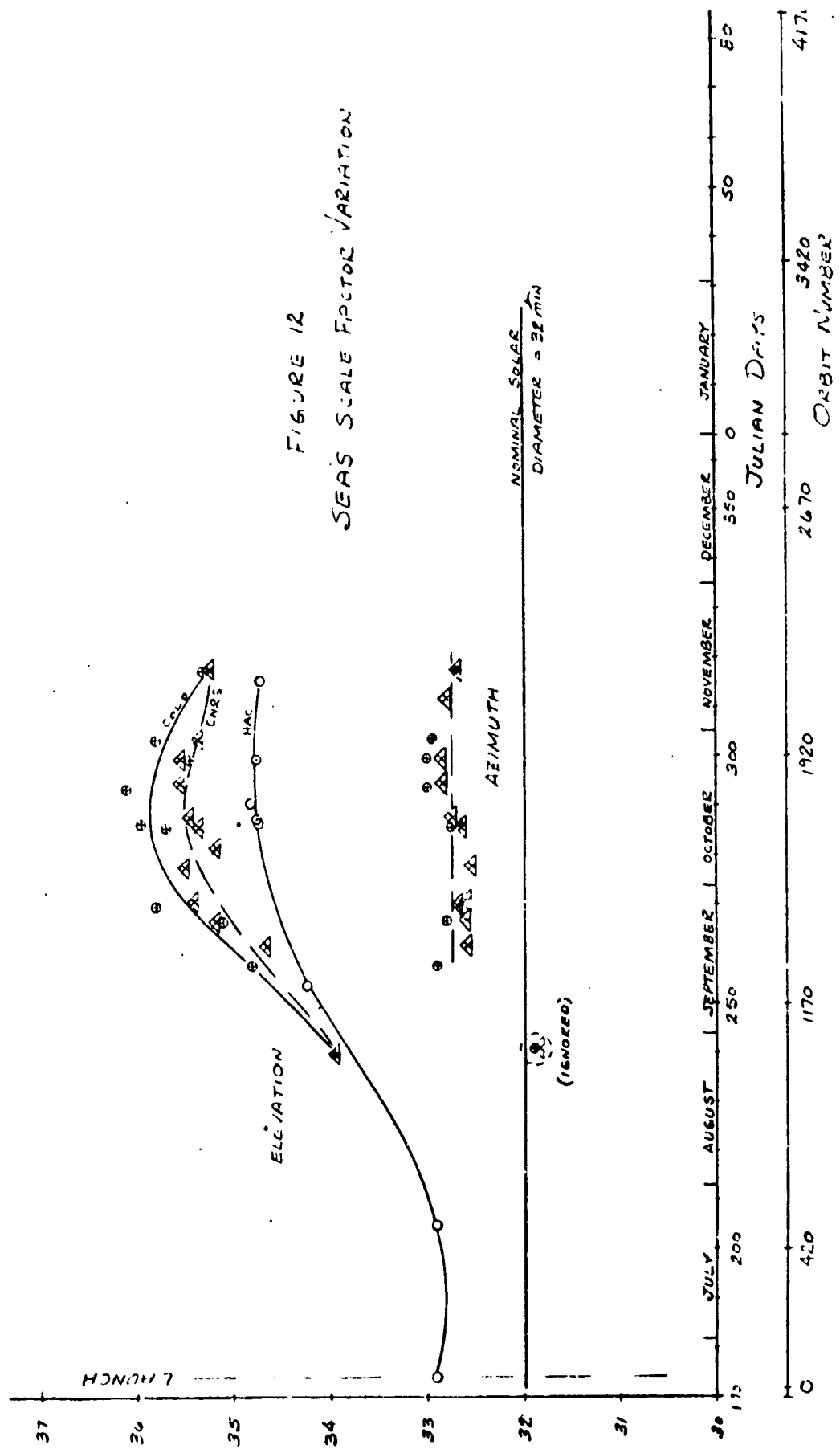


FIGURE 12
SEAS SCALE FACTOR VARIATION

shows a plot of the battery number 1 temperature sensors at that time. The 11-cell packs are located next to the rim panel. For this reason their temperature fluctuates more over a complete orbit than the 10-cell packs which are located approximately midway between the rim panel and the DBA hub.

Battery voltage, charge and discharge currents are also plotted in Figure 2 for battery number 1. The performance of battery number 2 is almost identical. This indicates that the two batteries are well matched, i.e., charge and discharge currents are shared evenly.

The power electronics units are performing in a nominal manner. Preregulator and experiment regulator output voltages are well within their specification requirements. The battery charge controllers recharge the batteries during the early part of each day period and then clamp the battery voltage at a suitable value, controlled by the temperature of the 10-cell packs. This effectively reduces charge current to the 0.2 to 0.4 ampere range at end of day to prevent battery overheating. The bus limiters are maintaining the bus voltages below 33 volts by absorbing all excess solar panel power. Only the four even numbered bus limiters are active -- those that dissipate heat in load resistors mounted on the S band ground plane antenna. The other four bus limiters will become active only if experiment loads become light or if some of the even numbered limiters fail.

The Wisconsin regulator tripped off during the ninth day in orbit. This appeared to be due to a temporary over-current condition in the experiment. No commands were sent to the spacecraft from the SCP or a ground station at that time. The experiment was turned on again with the same A regulator. The regulator and experiment continues to operate in a satisfactory manner.

Figure 15 shows a plot of all spacecraft currents for a full orbit. During day, the solar panel current divides between the observatory load and battery charge until the batteries are clamped. Excess panel current is then forced into the bus limiters. At night the sum of the two battery discharge currents is equal to the observatory loads.

Figure 13 Solar Panel Parameters (Orbit 591)

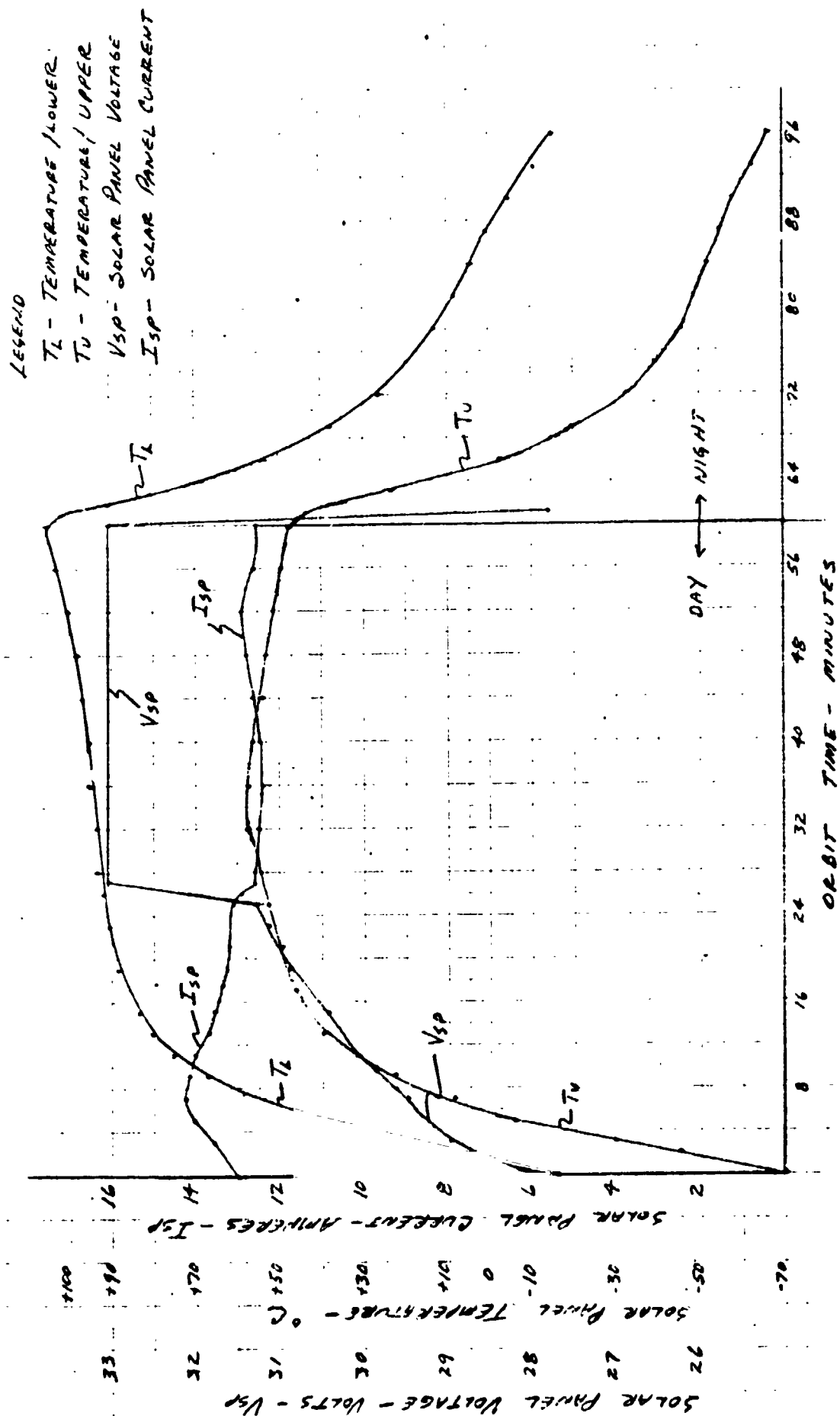


Figure 14 Battery Performance Parameters (Orbit 591)

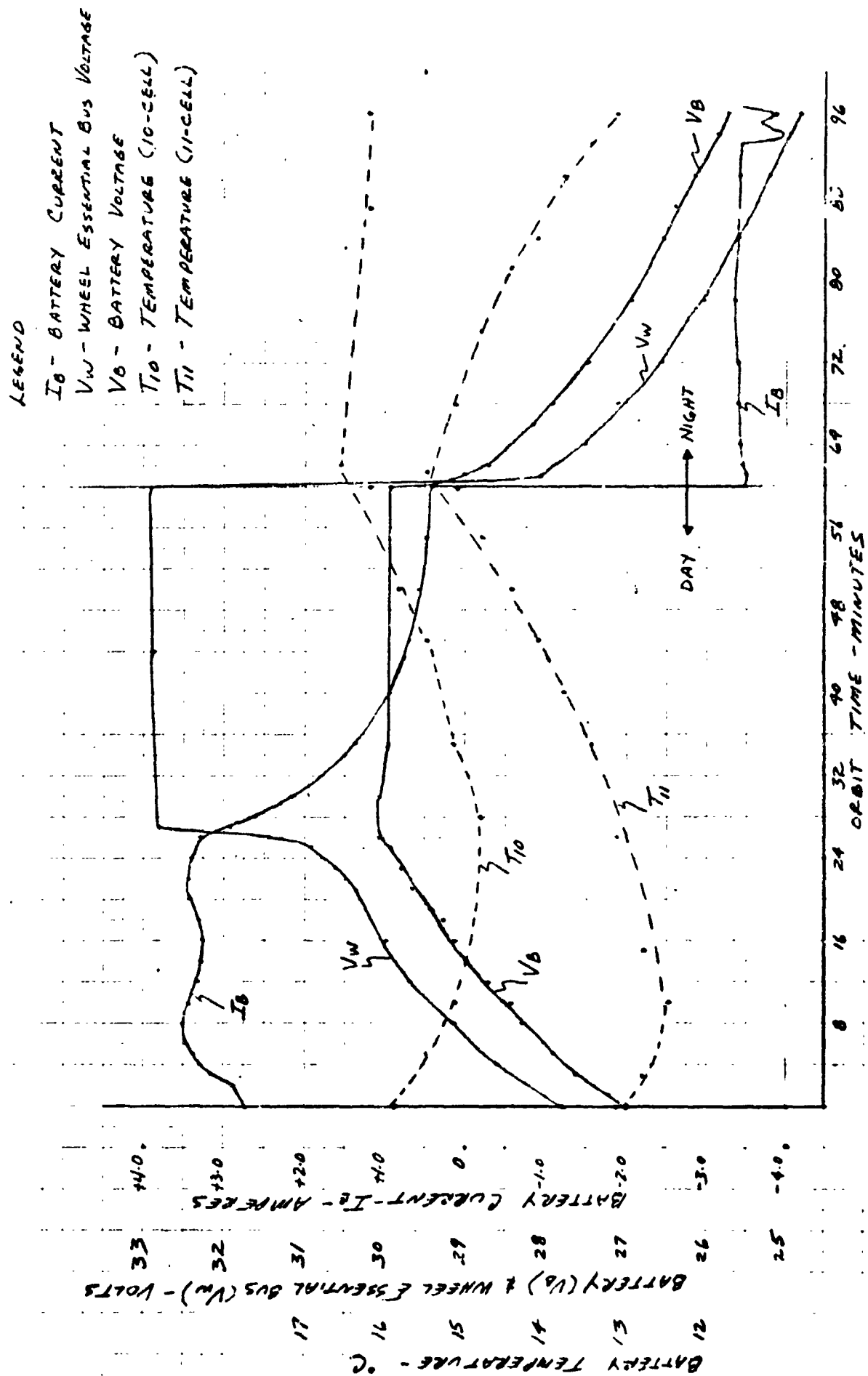
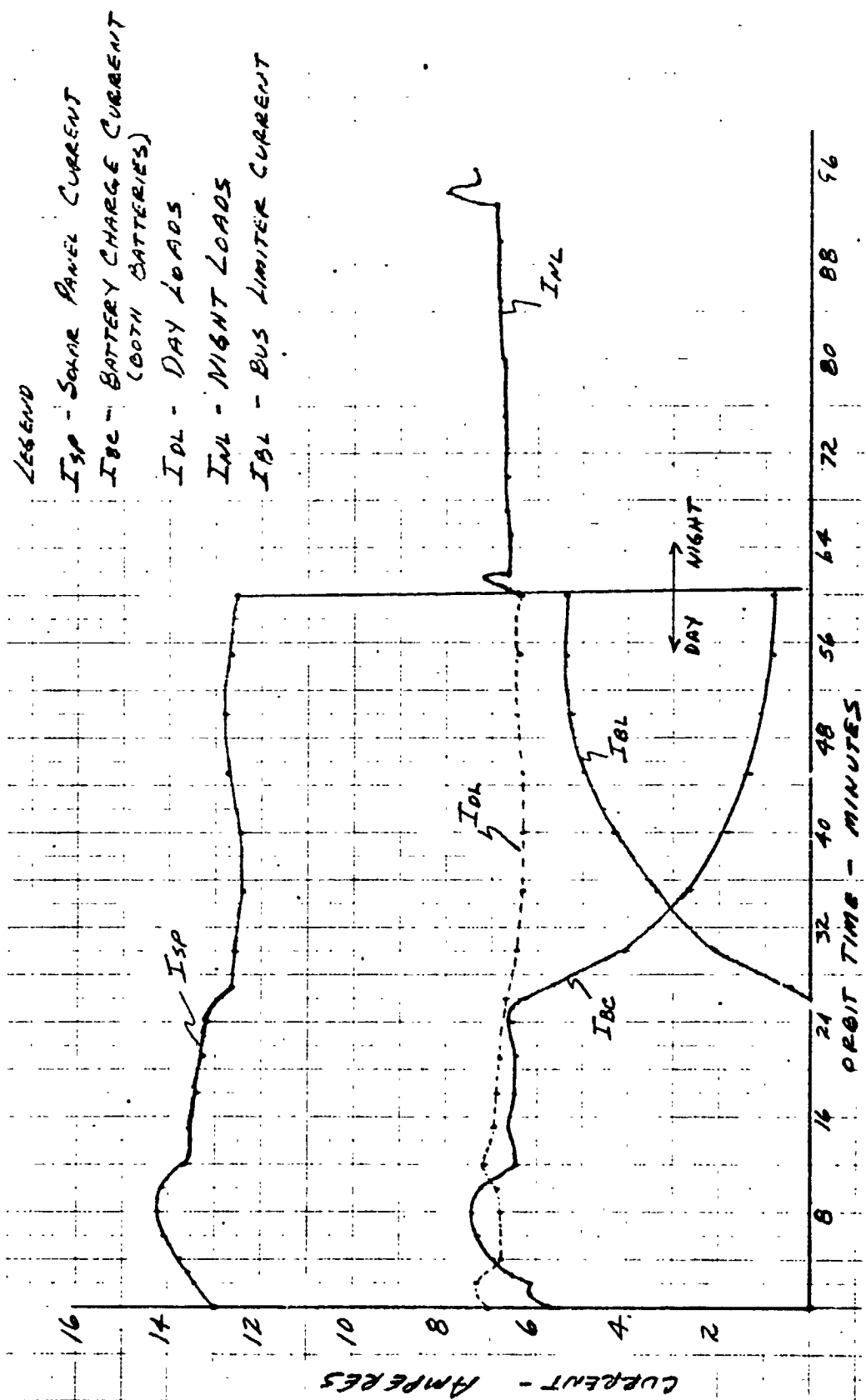


Figure 15 Spacecraft Loads (Orbit 591)



Thermal Performance

The thermal performance of the OSO-I Observatory for the initial 6 months in orbit is about as expected with the exception of the solar panel and DBA. The lower solar panel is running warmer than expected at its peak temperature of 109°C (expected was 107°C) while the upper portion of the solar panel is cooler at the end of eclipse than expected, -69°C measured, -59°C expected. Design operating limit for the solar panel is -65°C to 125°C with qual values of $\pm 10^\circ\text{C}$ added. During the sail thermal balance test solar panel temperatures of -68°C and 110°C were measured. The maximum measured DBA temperatures of 23 to 29°C exceed expected values by 1°C at the aft bearing to 4°C at the ECRA. These temperatures are below the DBA design limit of 30°C. (Qual limit is 40°C.) Table 2 compares the temperature range observed during this period in orbit of many of the subsystems with the expected temperature band for the orbital life of the observatory. The maximum battery temperature was observed to be 23°C while the temperature difference between packs and batteries remained less than 3°C and 5°C respectively. See Figure 19. As indicated previously the DBA thermal performance is about as expected while the ΔT across the bearings is approximately 2 or 3 degrees, $\leq 15^\circ\text{C}$ is the requirement. EDA temperatures were observed to be within the expected temperature range while ΔT from the inner race to the outer race measuring 1°C. This value is well within the required 15°C.

With the approach of Winter Solstice and corresponding short eclipse lengths of 24 minutes it appears that temperatures of many of the subsystems will exceed predicted values from 5 to 8°C. Although some of these subsystem temperatures are expected to exceed design limits none are expected to reach qual limits.

Closer monitoring of the spacecraft pitch angle to maintain it within the $\pm 4^\circ$ constraint and reduction of the S band transmitter operational duty cycle from 100% to 10% will minimize expected maximum temperatures. This expected over temperature condition is presently under study.

Figure 16 shows the thermal response of the solar panel during day 227 (fifty-five days after launch). The profile is as expected and is consistent with a 30 minute eclipse. The thermal performance of shear webs, rim panel and forward and aft closeouts for this day have also been included. The shear

web profiles (Figure 17) and the rim pan and forward and aft closeout profiles (Figure 18) are as expected and agree closely with data obtained during the OSO-8 observatory test performed at Hughes in March 1975. Figure 20 is a plot of an equipment shelf thermal response.

Since the thermal performance of the observatory tends toward the warm side there is no plan at this time to exercise any of the on-board heaters (i. e. , DBA, gimbal saddle).

As of this date the thermal health of the observatory is excellent and is expected to remain that way during its operational life.

TABLE 2

COMPARISON OF MEASURED WITH EXPECTED TEMPERATURES
(First sixty days in orbit) °C

SUBSYSTEM	EXPECTED BAND (including uncertainty)	MEASURED BAND (c)	DESIGN LIMITS (mounting surface)
Bus Limiters	6 to 33	11 to 32	-10 to 38
Charge Control	7 to 27	18 to 25	-10 to 38
VHF Transmitters	6 to 29	15 to 26	-10 to 38
S-Band Transmitters	0 to 42	13 to 40	-10 to 38
Tape Recorder Head	6 to 26	13 to 23	-10 to 30
Star Sensor Telemetry DBA	7 to 31	11 to 17	-7 to 38
Fwd. B inner/outer	6 to 25	20/16 to 28/23	-7 to 30
Aft. B inner/outer	7 to 25	20/18 to 26/24	-7 to 30
ECRA	8 to 25	21 to 29	-7 to 30
Motor	8 to 23	21 to 26	-7 to 30
Antenna Skirt	-32 to 82	-17 to 35	-65 to 115
Magnetometer			
Elec	2 to 33	13 to 33	z 4 to 38
Sensor	14 to 42	10 to 26	-20 to 38
N ₂ Tanks	6 to 31	13 to 26	-10 to 38
Methane Tanks	8 to 30	15 to 25	-10 to 38
Wheel Control Power Unit	4 to 24	15 to 27	4 to 38
Wheel Control Signal Unit	10 to 39	19 to 40	4 to 38

TABLE 2

COMPARISON OF MEASURED WITH EXPECTED TEMPERATURES
(First sixty days in orbit) °C

SUBSYSTEM	EXPECTED BAND (including uncertainty)	MEASURED BAND (c)	DESIGN LIMITS (mounting surface)
Shear Webs			
1	4 to 28	13 to 24	-10 to 38
2	4 to 27	11 to 22	-10 to 38
3	3 to 28	11 to 23	-10 to 38
4	10 to 29	15 to 24	-10 to 38
5	-3 to 28	4 to 23	-10 to 38
6	11 to 30	10 to 27	-10 to 38
7	-1 to 27	13 to 23	-10 to 38
8	4 to 25	13 to 23	-10 to 38
9	8 to 31	15 to 23	-10 to 38
Battery 1	4 to 24	12 to 23	0 to 25
Battery 2	4 to 24	12 to 23	0 to 25
Solar Panel			
Upper	-59 to 67	-69 to 63(a)	-65 to 125
Lower	-18 to 107	-12 to 109	-65 to 125
Sail Equipment Plate 1	-3 to 29	2(d) to 23	-7 to 49
Sail Equipment Plate 2	-3 to 29	20 to 30	-7 to 49
Sail Control Power Unit	See Footnote 1	10 to 27	-7 to 49
Sail Control Signal Unit	See Footnote 2	13 to 39	-7 to 49
SEAS Elec. (CNRS)	See Footnote 3	20 to 27(b)	-7 to 49
SEAS Elec. (COLO)	See Footnote 3	20 to 28	-7 to 49

TABLE 2

COMPARISON OF MEASURED WITH EXPECTED TEMPERATURES
(First sixty days in orbit) °C

SUBSYSTEM	EXPECTED BAND (including uncertainty)	MEASURED BAND (c)	DESIGN LIMITS (mounting surface)
Gyro Electronics	30 to 44	36 to 39	
Gyro	63 to 67	65	
ARA Baseplate	20 to 34	22 to 27	20 to 43
ARA Radiator	16 to 30	16 to 21	
Gimbal Saddle	8 to 33	19 to 30	10 to 30
Yoke			
Top	7 to 34	19 to 30	4 to 38
Bottom	4 to 30	3 to 24	4 to 38
Nutation Damper	0 to 24	-4 to 19	-18 to 38

Footnote 1: Temperature sensors in these units can read as much as 20°C above the equipment plate 1 temperature.

Footnote 2: Temperature sensors in these units can read as much as 25°C above the equipment plate 2 temperature.

Footnote 3: Temperature sensors in these units will be $\leq 5^{\circ}\text{C}$ above the gimbal saddle temperature.

- (a) Add 14°C to obtain Solar Cell Temperatures
- (b) Temperatures prior to SEAS A Electronics failure
- (c) With the exception of the shear webs, values noted are unit temperatures.
- (d) Saturated value. Actual temperature predicted to be -1°C . (See Figure 20).

Figure 16 Measured Solar Panel Thermal Response Day 227
Eclipse Length = 30 Minutes

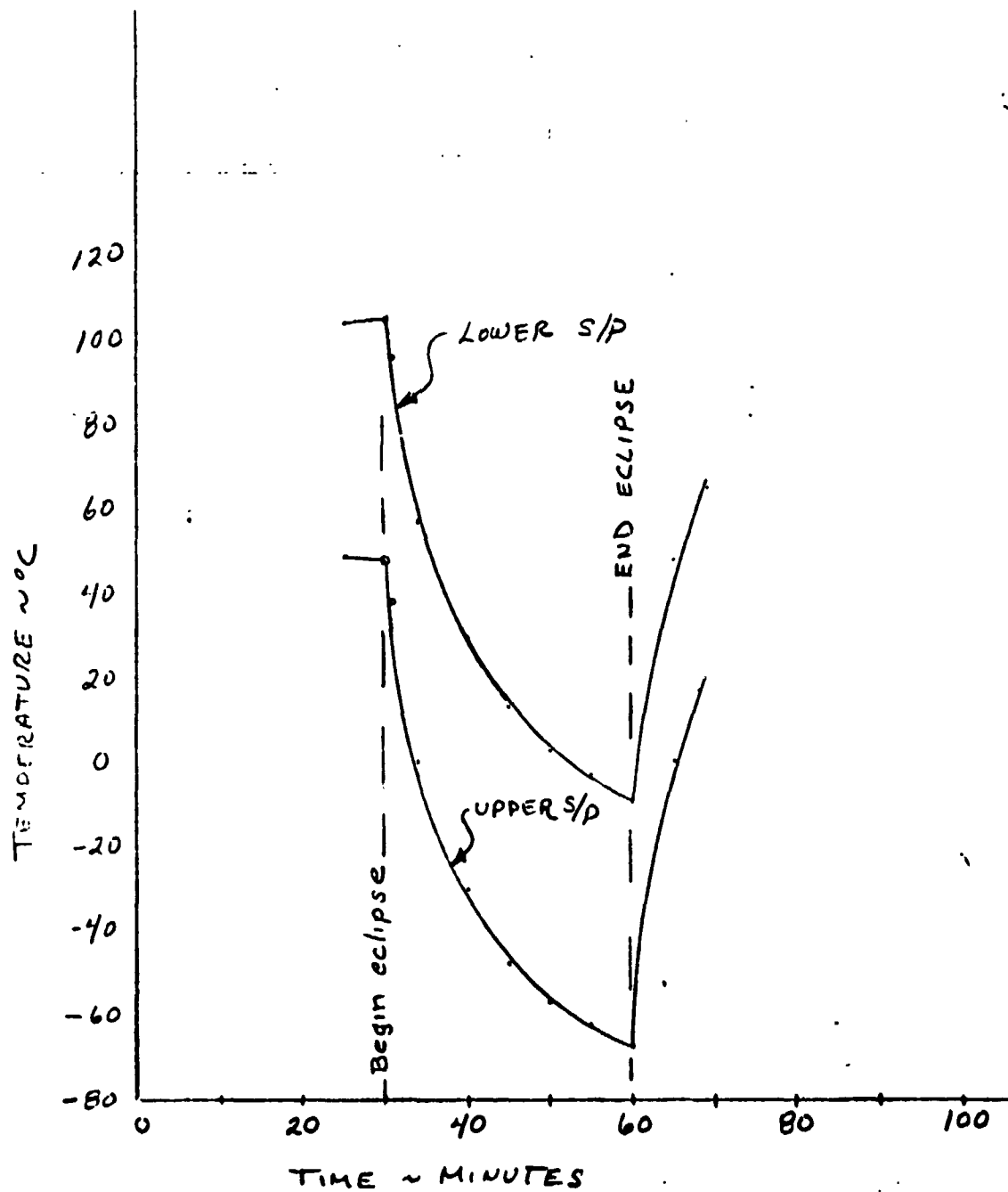


Figure 17 Measured Shear Web Thermal Response Day 227

Eclipse Length = 30 Minutes

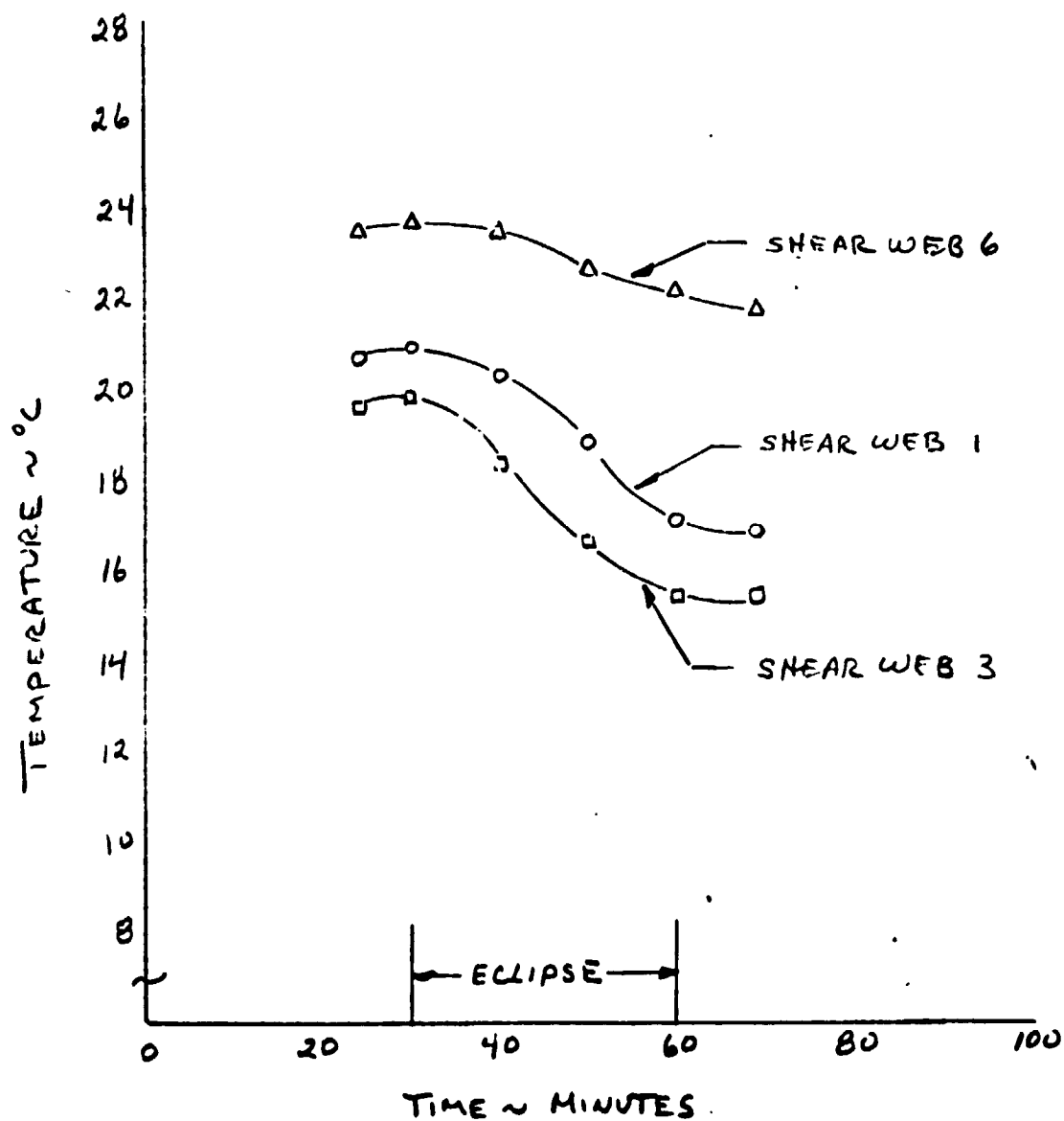


Figure 13 Thermal Response of Rim Panel and Closeouts
During Day 227

Eclipse Length = 30 Minutes

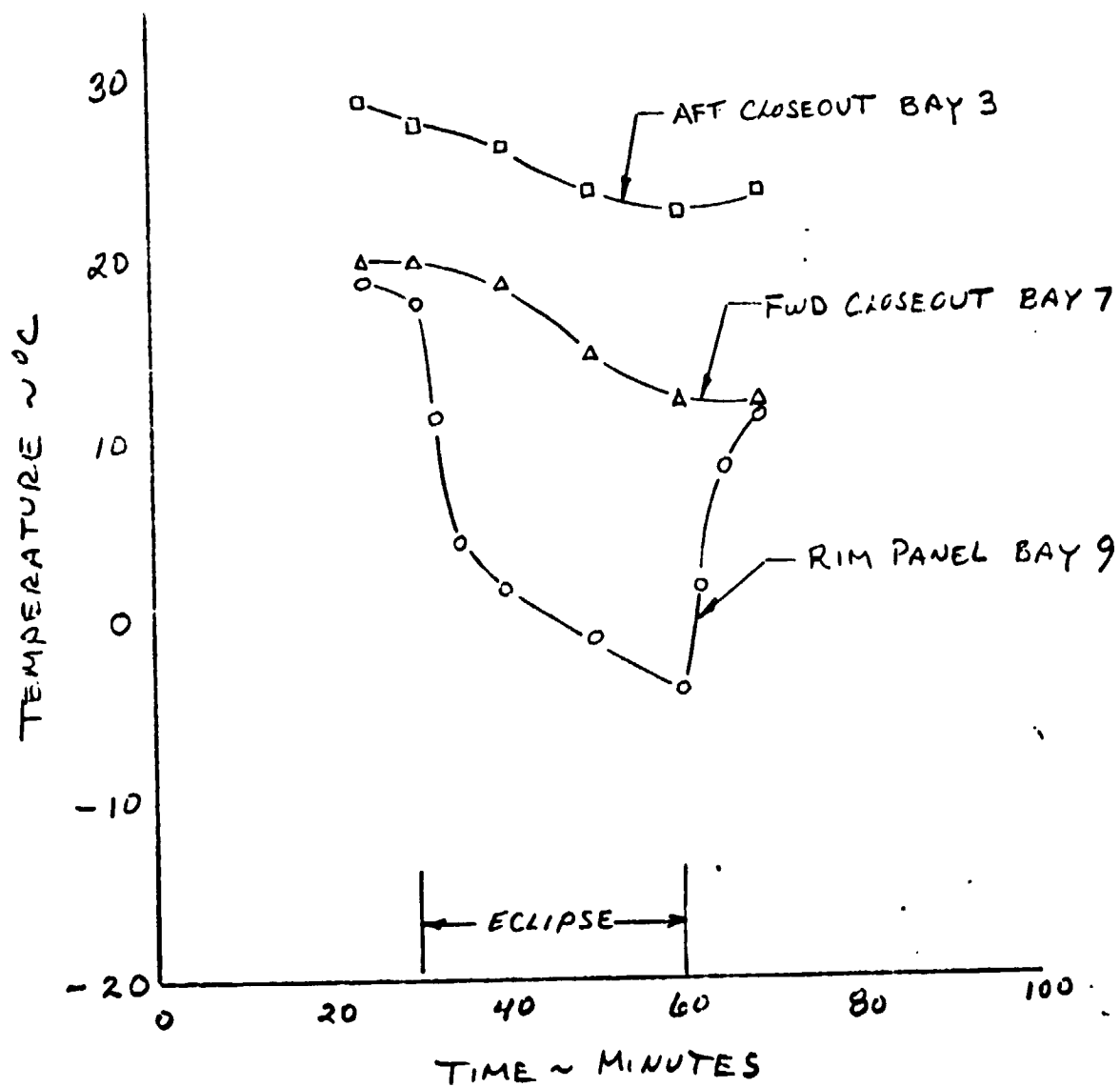


Figure 19 Batteries Thermal Response During Day 227

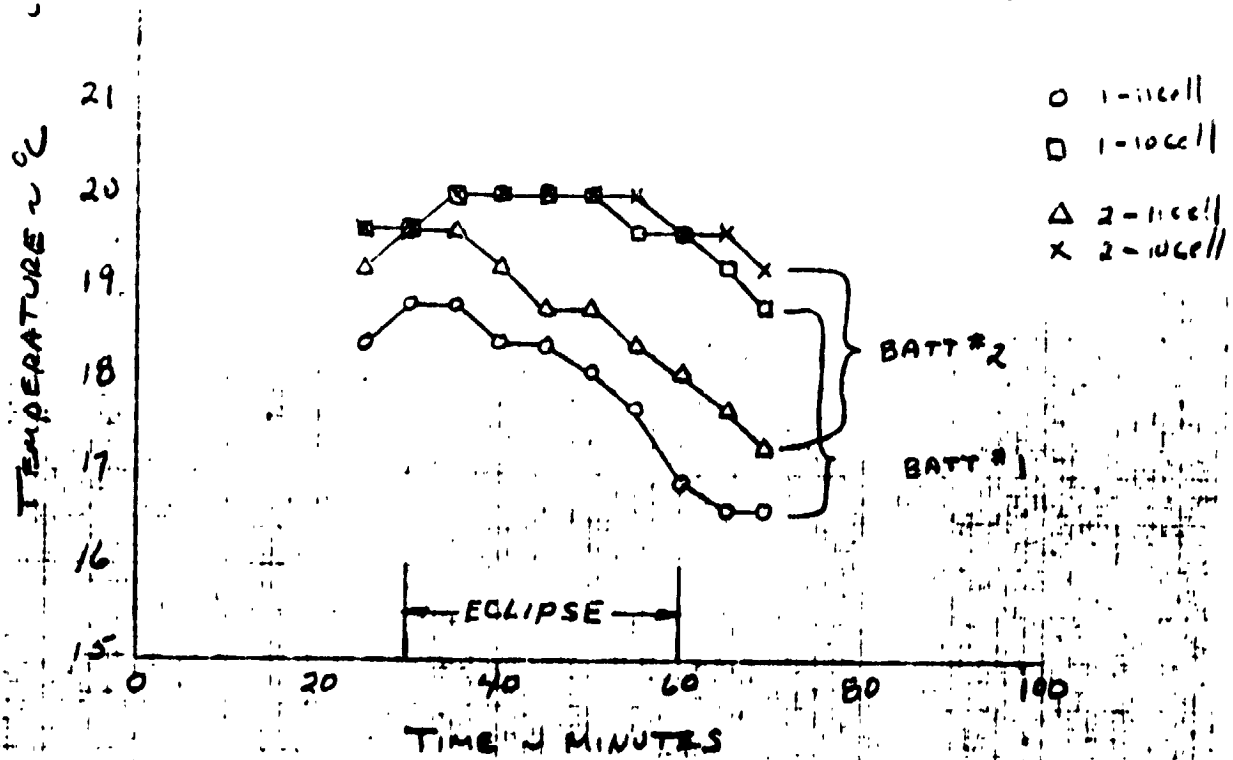
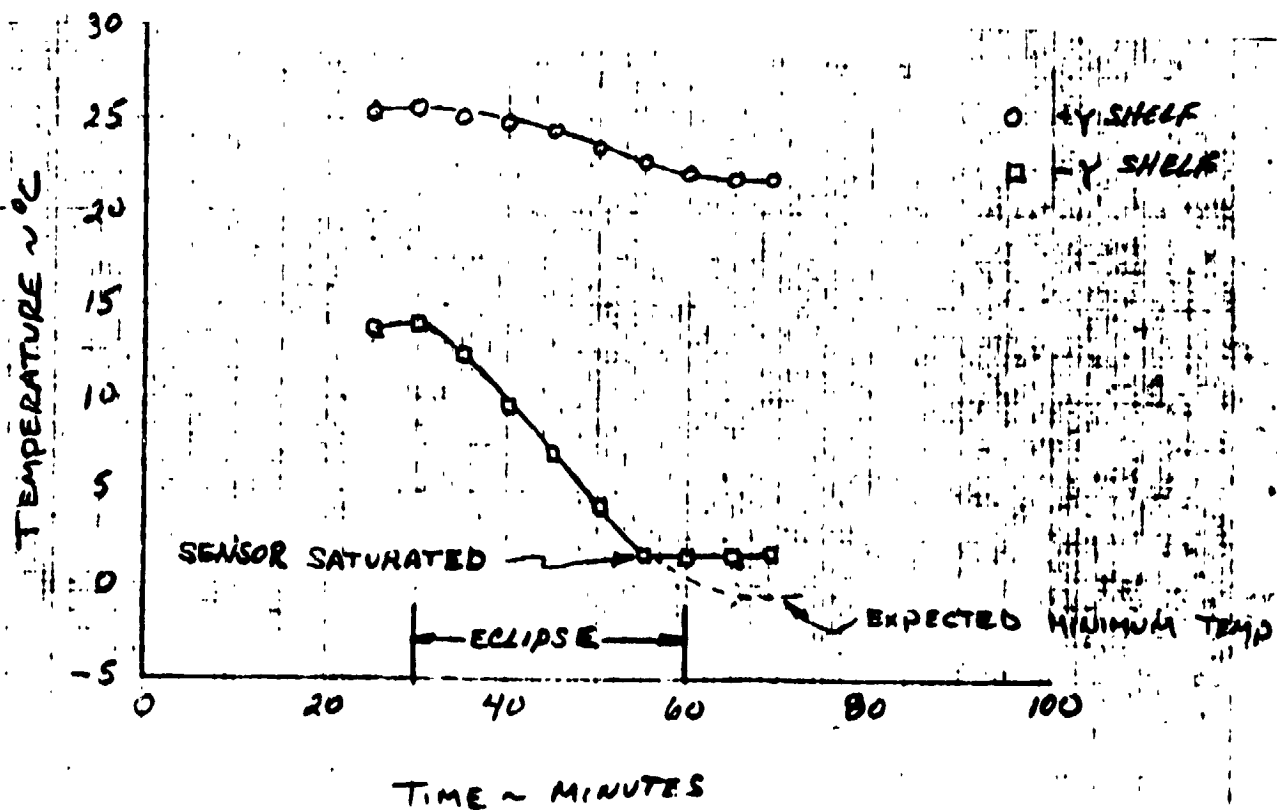


Figure 20 Equipment Shelf Thermal Response During Day 227



Telemetry and Command Subsystem

The telemetry and command subsystems continue to operate as designed after six months in orbit. No data has been lost due to spacecraft anomalies and no spurious commands have been executed. Three ground operational problems have been encountered: (1) readout of the Colorado junior memory utilizing the dwell mode, (2) tape recorder management program to minimize reaching beginning/end of tape, and (3) receiving real-time data via S-band.

The dwell mode problem has been resolved by changing the ground receiver loop bandwidth from 30 to 100Hz as was determined during pre-flight system testing.

The initial solution to the tape recorder management problem was to use only recorder B because it had the proper fix to allow beginning/end of tape to occur without problems. The management problem was resolved by programming the record and playback times via the SCP.

Receiving real-time data via S-band was achieved by reducing the station receiver bandwidth such that lock could be maintained on the carrier and not a sideband.

The stored command processor (SCP) was turned on and checked out, using memory A, during early orbital operation, orbit 17. The first mission sequence was loaded and started commanding the spacecraft and experiments, Colorado and CNRS, during orbit 30. New command sequences have been formulated and loaded every 6 to 24 hours. The SCP continues to operate properly, sending commands as expected.

The spacecraft has been operating with the "A" units, so SCP operation with the "B" units, including memory B, has not been checked out. Also, memory verification has been performed using VHF dwell mode, so S-band memory verification has not been checked out. SCP input commands and events which have been received and verified are shown in Tables 3 and 4

Table 5 lists the units which were exercised via the command subsystem during this report period.

TABLE 3
EVENT FLAG VERIFICATION

EVENT FLAG	FLAG TITLE (Subsystem Source)	VERIFIED
1	N. A.	
2	1M Autorestore Bus (Command)	
3	Day Event (Wheel Control)	YES
4	Flare Detection (LMSC)	YES
5	Flare Start (Columbia)	
6	SA Anomaly Strat (Frost, Boldt)	YES
7	CU Event A (Colorado)	
8	SA Anomaly Stop (Frost Boldt)	YES
9	CU Event B (Colorado)	
10	CU Event C (Colorado)	
11	Sail AZ Scan Stop (CNRS)	
12	Night Event (Wheel Control)	YES

TABLE 1
COMMAND VERIFICATION

COMMAND TITLE		CODE	VERIFIED
1.	SCP ON	8-32 24-32	YES
2.	SCP OFF	8-33 24-33	YES
3.	TRANSFER CMD	8-72 24-72	
4.	S-BAND DUMP ON	8-34 24-34	
5.	S-BAND DUMP OFF	8-35 24-35	
6.	RESET EVENT TM	8-36 24-36	YES
7.	INH CMD PROC	8-37 24-37	YES
8.	ENABLE CMD PROC	8-38 24-38	YES
9.	INH EVT PROC	8-39 24-39	YES
10.	ENABLE EVT PROC	8-40 24-40	
11.	FG A SEL	8-43 24-43	
12.	FG B SEL	8-44 24-44	
13.	DISABLE NON-CRIT	8-42 24-42	YES
14.	PC A. SEL	8-45 24-45	YES
15.	PC B SEL	8-46 24-46	
16.	ENABLE NON-CRIT	8-41 24-41	YES
17.	DATA MOD NEWVAL	8-73 24-73	YES
18.	SELECT MEM A.	8-12 24-12	
19.	SELECT MEM B.	8-13 24-13	

TABLE 5

UNITS EXERCISED

UNIT	A	B
VHF TRANSMITTERS	X	X
S-BAND TRANSMITTERS	X	X
FORMAT GENERATORS	X	
WHEEL PCM ENCODERS	X	
SAIL PCM ENCODERS	X	
WHEEL MULTIPLEXERS	X	
SAIL MULTIPLEXERS	X	
WHEEL CLOCKS	X	
SAIL CLOCKS	X	
TAPE RECORDERS	X	X
WHEEL SQUIB DRIVERS	X	X
SUN SQUIB DRIVER	X	X
CMD RECEIVERS	X	X
DEMOD/DECODERS	X	X
SCP/MEMORY	X	
REMOTE DECODERS	X	
OGRA HEATERS	X	X
OGRA	X	
DBA and EDA MOTOR	X	
WHEEL and SAIL SUN SENSORS	X	
PIA SUN SENSORS	X	X
SAIL CONTROL ELECTRONICS	X	
WHEEL CONTROL ELECTRONICS	X	
STAR SENSOR	X	N. A.
MAGNETIC TORQUER	X	N. A.
MAGNETOMETER	X	N. A.

TABLE 5
Continued

UNIT	A	B
POWER		
CHARGE CONTROLLERS	X	X
BUS LIMITERS	X	N. A.
PREREGULATORS		
SAIL	X	
WHEEL	X	
REGULATORS		
SAIL	X	
WHEEL	X	
CURRENT SENSORS	X	N. A.
OVERLOAD CONTROL	X	
DBA HEATERS		
GIMBAL SADDLE HEATER		

PROGRAM HISTORY

On 13 January 1971, Hughes Aircraft Company received official "go-ahead" by the award of a cost plus fixed fee contract NAS5-11390 for the conduct of a four (4) month study for the design definition of the OSO-I Spacecraft/Experiment Interfaces for the OSO-I mission. This effort was completed on 14 May 1971 at which time Hughes was awarded the Cost Plus Award Fee Contract NAS5-11400 for the design, development, fabrication, quality and reliability assurance, experiment integration, observatory testing, launch and post-launch support for three (3) Orbiting Solar Observatories; Protoflight/OSO-I, Flight OSO-J and K. On 19 November 1973 by contract modification No. 51 to contract NAS5-11400 NASA officially terminated, for the convenience of the government, OSO-J and K Flight spacecraft. Subsequently, as a result of fiscal funding constraints imposed by NASA on the OSO-I program, Hughes Aircraft Company and NASA agreed to complete performance of the OSO-I Observatory on a 70/30 cost sharing basis with cost ceiling in lieu of the original Cost-Plus Award Fee Contract. This agreement was entered into on 11 January 1974 as set forth in Contract Modification No. 53 to Contract NAS5-11400.

Figure 1 shows the OSO-I Master Schedule that was accomplished from January 1973 through launch on June 21, 1975.

The following is a brief summary of the problems encountered during system testing of the OSO-I Observatory:

Remote Multiplexers

Four multiplexers were removed from the Observatory for replacement of IC's. The failures were caused by static discharge created by the low humidity clean room. When the cause was found, all personnel were required to wear wrist-stats connected to observatory ground. Once this procedure was followed there were no further occurrences.

Battery Charge Controller

An oscillation problem developed between the two controllers after integration into the Observatory. Filtering was added into the interconnecting harness to solve the problem.

Magnetic Tape Recorder

During test of a similar tape recorder on another program it was found that the timing circuitry at end-of-tape (EOT) and beginning-of-tape (BOT) changed such that a mechanical relay received a pulse that was sufficient to open the relay but not close it ending up in a position midway causing complete failure of the recorder. Although this situation had a remote probability of occurring one of the OSO recorders was modified to preclude this unlikely occurrence.

PIA Sun Sensor

A number of relatively minor problems with the SEAS and its electronics have been encountered during this period, all prior to the start of environmental testing. They fall into three categories; induced failure, fabrication/integration errors, and design sensitivity. For example, the backup mode for capture involves slewing the sail by using the gyro to establish the slew rate and the SEAS to detect and lock on to the sun signal, stopping slew within the SEAS field of view. Capture from a slew rate of some 2°/sec was required by specification, because capture would occur too late resulting in oscillation without closing to null position. The requirement for this mode was determined not to be critical and the maximum slew rate for capture was reduced to 0.9°/second.

Star Sensor (GFE)

A removal of the signal processor for rework of a loose feed-through connector was accomplished prior to environmental test.

The following problems were encountered by the experiments during the system testing of the OSO-I Observatory:

Boldt Cosmic X-Ray Experiment

Two problems were experienced by the Boldt experiment. The first is the pickup of 3.2 KHz clock noise in the "A" detector electronics. This acts as if extra counts are being received by the detector. Since the total count capability is 100,000 counts, the principal investigator elected to live with the 3.2K "error". Lack of RF shielding in the vicinity of the clock lines internal to the experiment has been identified as the primary cause of the pickup.

The second problem, a noisy C-Detector high voltage power supply, was encountered just after initial experiment turn-on in thermal vacuum. Within 30 minutes the noise had decreased in a typical outgassing curve down to essentially normal levels. Operation of the power supply and detector remained normal for the balance of thermal vacuum. The principal investigator felt the power supply probably is normal and was turned on too early in thermal vacuum.

CNRS High Resolution UV Spectrometer Experiment

The CNRS experiment experienced two problems of significance. The least significant was a short corona experienced in the Lyman Alpha Hi-Voltage power supply shortly after turn-on in thermal vacuum. The noise cleared in roughly 5-6 minutes.

A second and more significant problem was that CNRS triggers Event Flag No. 11 into the SCP whenever night is sensed by the day/night sensor and CNRS is configured in the day mode. The day/night signal reconfigures CNRS, turning off its high voltage power supplies. This experiment reconfiguring apparently looks like detection of the night star pattern to CNRS logic circuitry and it sends out Event No. 11 to the SCP to start star field scan. This appears to be a normal characteristic of the spectrometer design and CNRS accepted it as is. A mission constraint has been entered to have

no operational commands in the SCP for Event No. 11 when going into night and to have CNRS reconfigured into night mode or off prior to going into night when Event No. 11 commands are desired.

Columbia Graphite Crystal X-Ray Experiment

Several problems were encountered by Columbia in thermal vacuum and in post-thermal vacuum performance testing. First, Hi-Voltage Power Supply No. 1 experienced varying voltage levels, going both low and high.

Second, the problem of positioning the internal calibration sources with the stepper motors returned. Columbia judged the problem to be software related.

Third, a detector rise time discriminator did not appear to work properly at hot (warm) temperatures with the high energy (Fe_{55}) external source. Yet, it functioned normally with the lower energy internal sources throughout the temperature range. This would suggest proportional counter no. 1 probably had experienced a gas lead.

The no. 1 counter and power supply were replaced prior to launch.

Frost High Energy Celestial X-Ray Experiment

The Frost experiment had two identified failures or malfunctions. The first is in the data system. It is evidenced by the loss of the second most significant bit in each data word. The problem was found to be a faulty buffer IC.

A second malfunction of Frost was the failure of the South Atlantic Anomaly PMT, apparently as a result of vibration. Since the Frost experiment has other means of detecting SAA and the spacecraft has a number of methods, it was the recommendation of the principal investigator that the experiment be flown with the PMT as is and turned off.

Lockheed X-Ray Heleometer Experiment

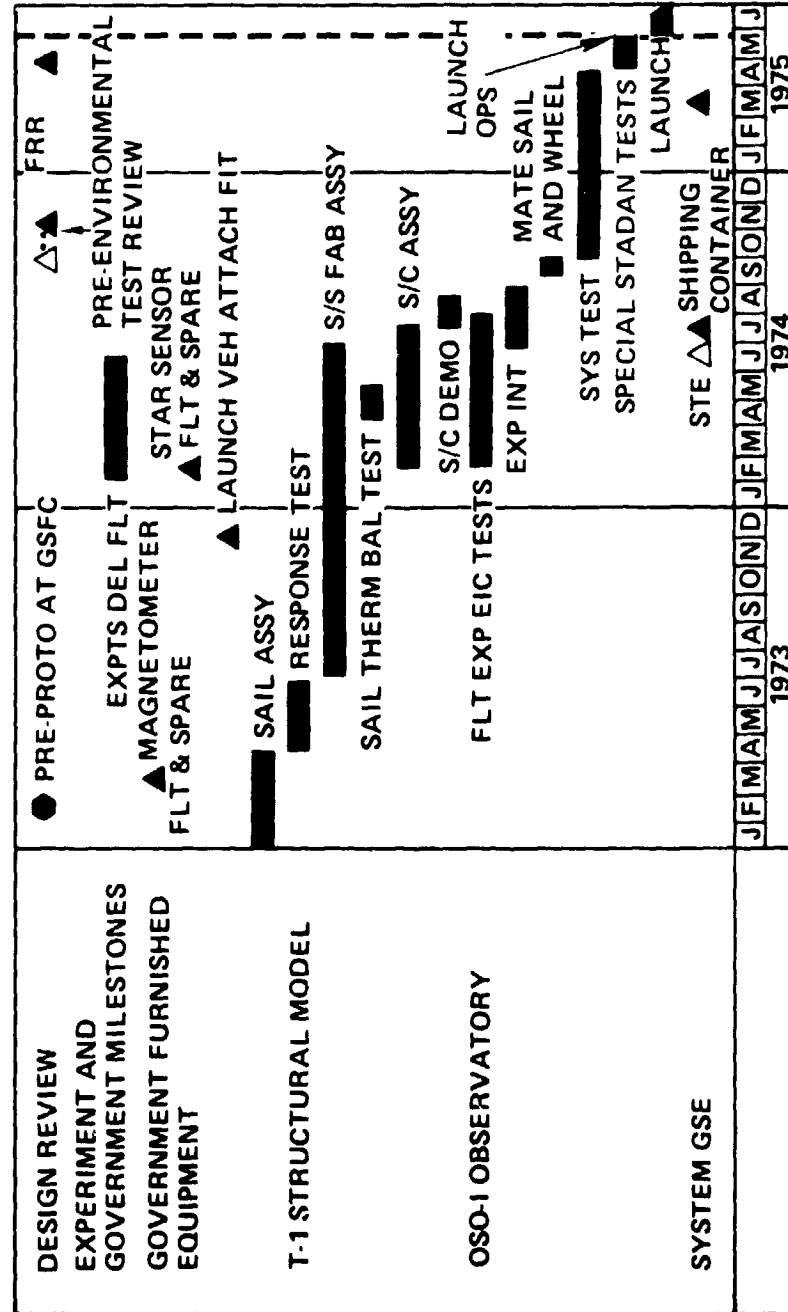
The one Lockheed problem occurred at low temperature in thermal vacuum. Below 10°C the Lockheed calibration sources do not step properly when commanded to do so. Lockheed indicated the stepping circuit was not adequately sized for temperature and the resulting problem was masked by another trouble during unit level testing of the experiment. No action was taken since the principal investigator felt he can live with the data he is receiving.

Wisconsin Soft X-Ray Experiment

The Wisconsin Experiment experienced instances of apparent "extra" SAE, MIP and major frame synch pulses. No comparable evidence on the space-craft side of the interface was identifiable. Some of the "extra" pulses affect only the special "self-test" logic circuitry in the experiment and will not affect the in-orbit data taking or results.

Two coronas were encountered in thermal vacuum, one due to improper configuration during pumpdown and the other too high a Torr during a special spin fixture test between Phase I and II of thermal vacuum.

OSO-1 MASTER SCHEDULE



56015-901

Figure 21